8-3-2018

# Efficacy of eluted antibiotics in 3D printed orthopaedic implants

Mohammed Mehdi Benmassaoud
*Rowan University*

# EFFICACY OF ELUTED ANTIBIOTICS IN 3D PRINTED ORTHOPAEDIC IMPLANTS

by

Mohammed Mehdi Benmassaoud

A Thesis

Submitted to the
Department of Mechanical Engineering
College of Engineering
In partial fulfillment of the requirement
For the degree of
Master of Science in Mechanical Engineering
at
Rowan University
April 20, 2018

Thesis Advisors: Shivakumar I. Ranganathan, Ph.D.
Tae Won B. Kim, MD.

## Dedications

It is my genuine gratefulness and warmest regard that I dedicate this work to my parents, my Aunt Latifa and Uncle Mark. Thanks to their support, I am the person who I am now and able to build a strong work ethic. Moreover, they never doubted in me. I also dedicate this thesis to my sister and my cousin Touria for believing in me no matter what the circumstance.

**Aknowledgements**

The success of this thesis is due to the constant support from the remarkable people. First and foremost, I would like to thank God for giving me the strength and persistence to finish my research. I place on record my grateful appreciation and beholden to my two advisors Dr. Shivakumar Ranganathan and Dr. Tae Kim for their constant guidance, encouragement, and patience to get my masters done. Their involvement is much appreciated. Special thanks to Dr. Jennifer Kadlowec for agreeing to be one of my thesis committee members and supervising my research in my last semester. I am thankful to Dr. Xue Wei to be in the committee.

I am very thankful to my two grandfathers and grandmother for having faith in me. Special thanks to my parents, Aunt Latifa, Uncle Mark for making me the person who I am now. I am also thankful to my sister, Uncle Adile, my cousin Touria, Aunt Faiza, Samira and Souad, my both sides of my family, and my friends for supporting me and encouraging me.

Special thanks to Jack Williams, Billy Peppers, Chris Kohama, Brandon Foltiny, Haley Schappell, Alec Salvatore, Theo Mercurio, Christian Beauvais and Muhamed Ridwan Murshed for their involvement in this project. I acknowledge Chris Kohama and Alec Salvatore for getting the results described in the second chapter of this thesis. Finally, I am grateful to the Mechanical Engineering department and the College of Engineering at Rowan University for giving me resources to run the experiments. I am thankful to Dr. Krumminacker for giving us space in his lab run the Kirby-Bauer tests. Lastly, special thanks to New Jersey Health Foundation for funding my research and TECOMET INC. for outsourcing Titanium implants for our research.

**Abstract**

Mohammed Mehdi Benmassaoud
EFFICACY OF ELUTED ANTIBIOTICS IN 3D PRINTED ORTHOPAEDIC IMPLANTS
2017-2018
Shivakumar I. Ranganathan, PhD and Tae Won B. Kim, MD.
Master of Science in Mechanical Engineering

Costs associated with musculoskeletal diseases in the United States account for 5.7 % of the Gross Domestic Product (GDP) [1]. As such, there is a need to pursue new ideas in orthopaedic implants that can decrease cost and improve patient care. In the recent years, 3D printing using Fused Deposition Modeling (FDM) or Stereolithography (SLA) has opened several exciting possibilities to create orthopaedic implants. Such implants can be engineered to release antibiotics in a controlled manner either by infusing the drug into the material during manufacturing or by using built-in design features such as micro-channels and reservoirs [2]. The use of heat in FDM and Ultra-Violet (UV) light in SLA could impact the anti-bacterial effectiveness of antibiotics. Furthermore, the ability of 3D printed orthopaedic implants to elute antibiotics, and the rate of elution are not well understood. The objective of this thesis is threefold: i) Evaluate the efficacy of antibiotics exposed to UV light and heat; ii) Conduct numerical and experimental studies to assess drug elution through implants and iii) Perform Kirby–Bauer testing to determine whether the eluted antibiotics from 3D printed polymer and metal implants with built-in features maintain their antimicrobial property. Results indicate that antibiotics elute in a controlled manner and remain effective. Furthermore, the implant geometry can be optimized using a computational model on drug elution calibrated with real world data.

## Table of Contents

## Table of Contents (Continued)

**Table of Contents (Continued)**

## List of Figures

## List of Figures (Continued)

## List of Figures (Continued)

## List of Tables

Table Page

# Chapter 1

## Introduction

Deep bone infections after orthopaedic surgery remain a difficult problem to treat. Although penetrance of antibiotic in bone is well documented, its levels and ability to sterilize the bone is not well understood [3]. Furthermore, the presence of a metal implant on which bacteria can grow and thrive makes it a challenge to eradicate the infection without removal of the implant and compromising structural stability or joint function [4-6].

Orthopaedic trauma patients who suffer open fractures and patients undergoing joint replacement surgery (hips and knees) are at high risk for developing post-operative surgical infections. Osteomyelitis, is treated with the removal of the implant, surgical debridement, and placement of a material, which acts as a delivery vehicle for high dose local antibiotics to the bone. The most commonly used material is Poly-Methyl Methacrylate (PMMA), or bone cement. The antibiotic of choice is loaded into the PMMA at the time the polymer and monomer are mixed, and then the material is fashioned into the necessary shape or size [7-10]. In orthopaedic trauma surgery, intramedullary rods are used frequently to act as internal splints in long bones such as the femur and tibia until the fracture heals. When a femoral or tibial rod is infected, treatment consists of removal of the rod, surgical debridement of the bone and placement of a temporary rod made of antibiotic loaded PMMA. Unfortunately, rates of failure are reported to be as high as 15 % [11-14]. Similarly, in joint replacement surgery, large articulating metal implants are utilized to treat osteoarthritis. The gold standard treatment is a 2-stage process whereby the implant is removed and temporarily replaced with a spacer made of PMMA with antibiotics. This spacer can be articulating or non-articulating. The patient receives a 6-8 week course of intravenous antibiotics, and then returns to surgery for a re-implantation of a new joint replacement. Unfortunately, even with this aggressive treatment regimen,

re-infection rates are as high as 15 % [15-19]. The use of PMMA as a drug delivery mechanism has the following problems–

(a) When used in joint replacement settings, patients are left non-weight bearing on the extremity for 6-8 weeks, frequently placed in casts and have problems with cement dislodging and bone erosion [20].

(b) Drug elution properties of PMMA have been shown to be poor [21,22]. The implant is also susceptible to bacterial colonization and becomes a nidus for continued infection [23-25].

(c) Polymerization reaction for PMMA is highly exothermic. This limits the antibiotics that can be mixed into the cement [26].

Thus, there is an inherent clinical need for new and improved drug delivery materials/implants, and 3D printing offers a potential solution to this problem. The antibacterial effectiveness of the antibiotics will be analyzed using Kirby-Bauer test [27].

### 1.1. Key Contributions

The key contributions of this thesis are as follows:

(a) Analyze the effect of 3D print settings (temperature and ultraviolet light) on the efficacy of eluted antibiotics.

(b) Conduct experiments to determine the drug elution from the implant using HPLC and use the results to validate numerical models.

(c) Study the release of antibiotics from poly-caprolactone (PCL), poly-lactic acid (PLA) and titanium grade Ti-6Al-4V femoral implants.

### 1.2. Overview of the Thesis

The key contributions will be discussed in the subsequent chapters. The effect of temperature and ultraviolet light on the efficacy of doxycycline, vancomycin and cefazolin will be discussed in chapter 2. Subsequently, experimental and numerical

studies will be conducted to investigate the drug elution through 3D printed polymeric box shaped implants in chapter 3, while femoral implants will be considered in chapter 4. Lastly, the overall summary, limitations and future work will be discussed in chapter 5.

# Chapter 2

## Effect of Temperature and Ultraviolet Light on Efficacy of Eluted Antibiotics

Fused Deposition Modeling (FDM) and Stereolithography (SLA) are two of the popular techniques used to print orthopaedic implants. To print a part, FDM uses high temperature to melt the filament as it passes through the nozzle, whereas SLA relies on an ultraviolet (UV) light. When the antibiotics are introduced in the material, high temperature and UV light can adversely affect the anti-bacterial effectiveness of antibiotics. In this chapter, we examine: i) the effect of high temperature and UV light on the efficacy of antibiotics and ii) composite resin made up of various weight fractions of Polyethylene Glycol (PEG) and Polyethylene Glycol Diacrylate (PEGDA) for SLA. Results indicate i) that even after exposing doxycycline, vancomycin and cefazolin at different temperature between 20 oC and 230 oC for 15 seconds, the antibiotics did not lose their effectiveness (kill radius of at least 0.85 cm). Whereas, vancomycin is sensitiveto UV light compared to doxycycline and cefazolin, ii) doxycycline was present in the mixture of PEG/PEGDA with highest efficacy found in a resin with 20 % PEGDA and 80 % PEG (1.8 cm of kill radius), whereas lowest efficacy was in 100 % PEGDA (1.2 cm of kill radius).

### 2.1 Introduction

In the recent years, 3D printing techniques have revolutionized the design of medical implants. For instance, Radenkovic et al. proposed 3D printing human hollow organs with lower architectural complexity such as arteries, trachea, larynx and many more anatomical applications [28]. Along similar lines, Mannoor et al. evaluated the possibility of 3D printing bionic ears. The authors printed the model by slicing the Computer Aided Design (CAD) model into layers with the help of the laser and inks

[29]. Furthermore, 3D printing has also found applications in dentistry. Tamimi et al. compared 3D printed monolithic monetite blocks and autologous onlay grafts for craniofacial vertical bone augmentation in rabbits. The authors conclude that the two methodologies both have the same efficacy on craniofacial bone augmentation. However, they consider the 3D printing method as an attractive alternative solution [30].

When dealing with knee and hip arthroplasty, Zhang et al. proposed the patient-customized computer tomography aided design (CAD) and low temperatures to 3D print a biphasic calcium phosphate cement spacer containing antibiotics for total hip arthroplasty. The results obtained suggested significant model-to-model variation between patients. However, the in-vitro and in-vivo experiments proved the feasibility of using 3D printed implants for hip arthroplasty [31].

Finally, Kim et al. proposed 3D printing knee implants using Poly-lactic-acid (PLA) instead of the PMMA bone cement. The authors took into consideration three parameters (infill percentage, reservoir volume, and the quantity of micro-channels for injecting the antibiotics inside of the polymer) when printing implants. Results showed the antibiotics eluted within a span of two weeks [32]. In conclusion, 3D printing techniques have shown to be a great success in orthopaedic surgery.

In the recent years, several materials have been used for 3D printing including plastics, ceramics, metals, or living cells [33]. There are several manufacturing techniques available for 3D printing. These include: i) Selective Laser Sintering (SLS) ii) Thermal Inkjet Printing (TIJ) iii) Fused Deposition Modeling (FDM) [34] and iv) Stereolithography printing (SLA). SLS relies on powder to print materials and used for printing metallic components [34]. TIJ focuses on the technology that relies on thermal, electromagnetic, and piezoelectric concept and uses an ink to print materials [35]. FDM relies on heating and extruding polymers to create printed parts

[34], while SLA utilizes liquid resin curing under UV light to generate a 3D print and are among the most popular 3D printing techniques.

We propose exploring the possibility of using FDM and SLA to 3D print orthopaedic implants. Thereby, we propose examining the effect of high temperature and UV light on the efficacy of doxycycline, vancomycin and cefazolin.

### 2.2 Hypotheses

In applying 3D printing in orthopaedic implants, we hypothesize the following:
a. Heat cycle/temperature does not degrade the efficacy of released antibiotics to a degree which renders them inert.
b. UV exposure (similar to SLA) does not degrade the efficacy of eluted antibiotics.

### 2.3 Evaluation of the Hypotheses

Fused Deposition Modeling (FDM) printing was one of the methods used to construct the implants. It involved heating the filament to its melting point and then extruding it onto the build plate layer by layer until the implant was fully constructed. Whereas, SLA printing relies on liquid resin that will cure when exposed to ultraviolet (UV) light. Through the 3D printing FDM process, the antibiotics infused into the material are irradiated by heat. However in SLA, the antibiotics are exposed to UV light. If these antibiotics degrade a significant amount through such exposure it would be futile to load them into a prosthesis. Thereby we propose using kill studies to investigate the effectiveness of the antibiotics heated at different temperature.

The bacteria used for the kill studies was prepared by first sterilizing a beaker of Lysogeny broth (LB) and pipetting out 4 mL into a 15 mL vial. Then an inoculating loop was swabbed onto the bacteria and then immediately swirled into the 15 mL vial of LB. The vial was then placed into an incubator for 24 hours. After

which enough bacteria had grown to be used in the experiment.

The kill studies procedures was as follows: first 1 L of Deionized (DI) water was mixed with agar powder, second was to heat this solution to near boiling, third was to pour the liquid agar until the surface of the petri dish had been fully covered, fourth was to let the agar cool and solidify inside the petri dishes, and finally was to seed the petri dishes with E. Coli K-12 strain. The seeding process was done by micropipetting 50 microL of bacteria broth onto each petri dish. If the petri dishes had been dried out to due storage conditions it's important to also pipet 50 microL of LB onto each plate along with the initial 50 µL of bacteria broth. Subsequently, the bacteria was evenly spread across the surface of the petri dish using an L-Shaped cell spreader.

The final step is to soak filter paper disks with 6 mm diameter in the solution retrieved from the experiments and were immediately placed on the petri dish following the seeding procedure. At the bottom of each beaker were paper towels soaked in water. Also the tops were loosely covered with seran wrap and the entire beaker was placed inside an incubator. This final step was done to prevent drying out of the petri dishes. Once the petri dishes were placed into the incubator for 24 hours they were removed and then analyzed using pictures and ImageJ. Fig. 1 shows the schematic of the kill studies.

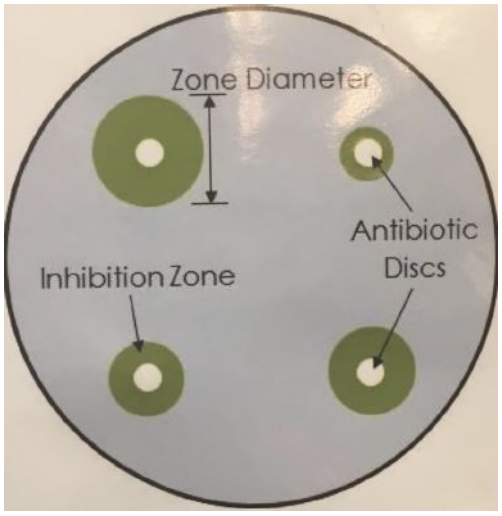


*Figure 1.* Schematic of antibiotic loaded filter disks in bacteria seeded petri dish.

**2.3.1 Effect of print temperature on the efficacy of eluted antibiotics** . The kill studies were done on doxycycline, vancomycin and cefazolin. Each of these antibiotics were tested between room temperature and 230 $^0C$ with an increment of 20 $^0C$. The zone inhibition for each antibiotic was detected and represented in the graph shown in Fig. 2.

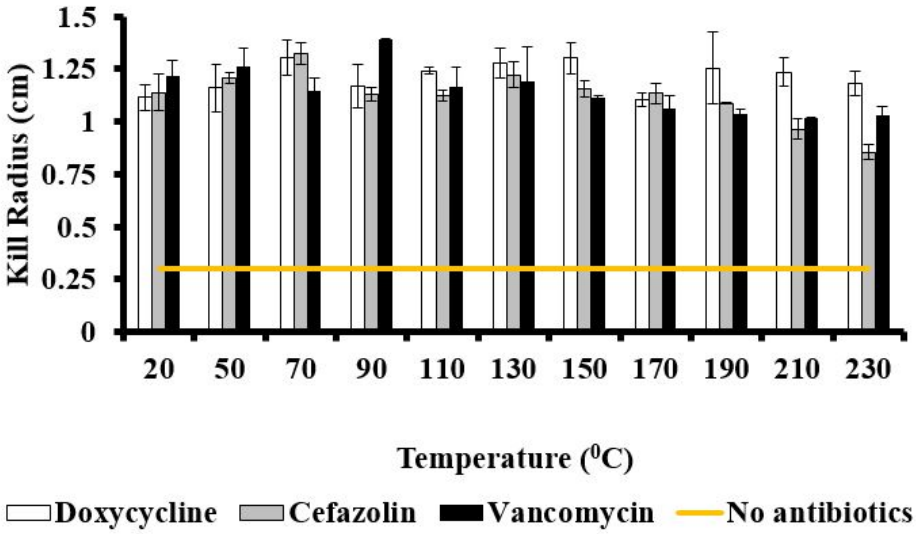


*Figure 2.* The kill radius of each antibiotic at different temperature.

The white, grey and dark columns represent the kill radii of doxycycline, cefazolin and vancomycin, respectively. The orange line represents the no zone inhibition situation (meaning when antibiotic lose completely its efficacy). The kill radius of each antibiotic is larger than the one with no zone inhibition. The no zone represents the case when the antibiotics lost their efficacy and represent the radius of the filter paper (0.3 cm). Therefore, the heat has no impact on doxycycline, cefazolin, and vancomycin. Indeed, Doxycycline has an average of 1.21 cm with 4.8 % confidence and standard error of 0.022, cefazolin has an average of 1.12 cm with 8.4% confidence with standard error of 0.038 and vancomycin has an average of 1.15 cm with 7.7% confidence with standard error of 0.035. These imply that the kill radii does not fluctuate deeply. The fluctuation happens due to the sample-to-sample error done in Kirby-Bauer test.

**2.3.2 Effect of ultraviolet light on the efficacy of eluted antibiotics**. Stereolithography (SLA) printing is appealing due to its ability to produce a solid product with a low temperature procedure when compared to the FDM process. In this process, the resin is exposed to highly concentrated UV light, which stimulates a photochemical reaction that results in the liquid mixture polymerizing, thus gaining the ordered structure of the solid [36]. The antibiotics Doxycycline, Cefazolin, and Vancomycin were exposed to wavelength of 400 nm for 10 hours and subsequently the efficacy was tested in Kirby-Bauer test. Fig. 3 shows the effect of UV wavelength of 400 nm for 10 hours considering the control at zero hour.

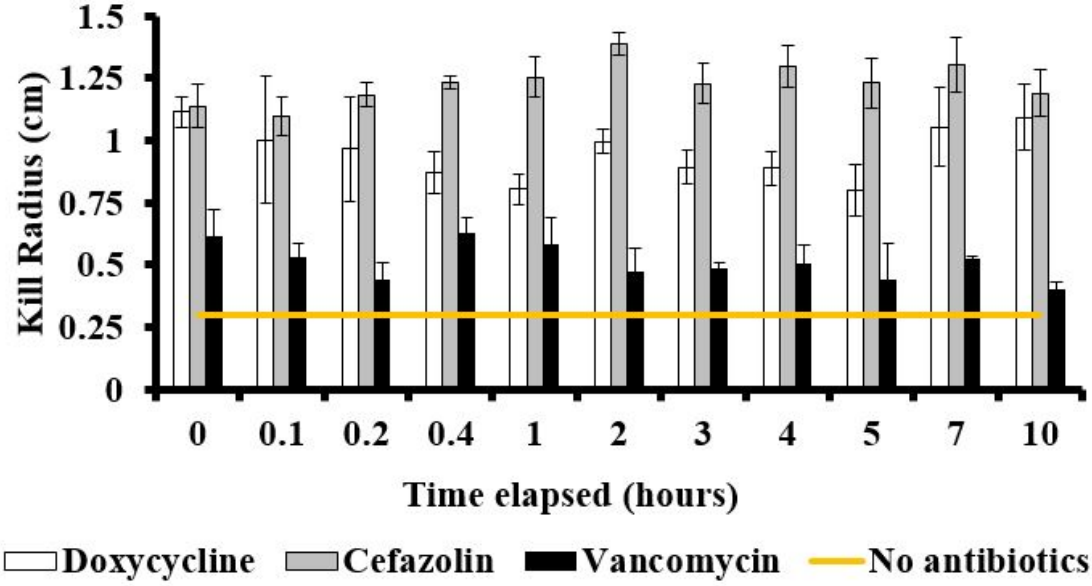


*Figure 3.* The kill radius of the antibiotic when exposed to UV wavelength of 400 nm for 10 hours.

As expected, cefazolin did not lose their effectiveness and still had antibacterial ability. However, doxycycline lost about 1.89% of its efficacy after 10 hours. Moreover, its mean radii is 14.5% less than the radius at control. In fact, the mean radii of doxycycline is 0.95 cm with standard error of 0.033 and the mean radii of cefazolin is 1.23 cm with an error of 0.024. These imply that cefazolin and doxycycline could be used and still be effective. In contrary, the longer vancomycin is under the UV light, the lesser is its kill radii. In fact, after 10 hours, it lost about 35% of it efficacy and its mean radius is 58% less than the one at control. Thereby, vancomycin is sensitive to UV light.

An experimental resin of Polyethylene Glycol (PEG) and Polyethylene Glycol Diacrylate (PEGDA) with a photoinitiator, diphenyl phosphine oxide, was formulated to produce 3D-printed objects. The PEG and PEGDA created the base structure of the polymer, while the photoinitiator stimulated crosslinks in the polymer when exposed to UV light, allowing the liquid to cure. A volume-to-volume resin containing 50% PEG, 50% PEGDA, and one gram of photoinitiator per 100 milliliters has been used for experimental purposes.

Cured resin samples were produced to determine physical and chemical processes of the crosslinked polymer. Among these properties, antibiotic elution was the most important. For this area, it was necessary to find a process that would be able to cure resin in a uniform manner. Attention was shifted to a new procedure in which a mold designed to prepare bone cement was repurposed to hold liquid resin. Above this mold, a UV lamp using the same wavelength as the SLA printer was positioned to shine down upon the liquid lying in the mold. The described apparatus can be seen in Fig. 4.

*Figure 4.* The mold and UV lamp apparatus used to cure resin without the use of SLA.

The bone cement mold contains seven identical channels that run parallel to each other. These channels were utilized to evaluate several different resin compositions to compare their properties. These different compositions were labeled in terms of PEGDA, which contains the functional group that allows the resin to be polymerized. The different compositions tested were 0% PEGDA, 20% PEGDA, 40% PEGDA, 60% PEGDA, 80% PEGDA, and 100% PEGDA, with the balance being comprised of PEG. Before the testing began, it was predicted that the 0% PEGDA sample would not cure at all, and the 100% PEGDA sample would contain the most crosslinks of any of the samples. It was also predicted that as the amount of crosslinks increased, the structural stability of the cured sample would increase and the elution of antibiotics through the sample would decrease.

After preparing the liquid resin using the compositions described above, five milligrams of Doxycycline were added per each milliliter of liquid solution for each sample. This antibiotic-infused resin was thoroughly mixed to create homogeneous samples, and these samples were then cured using the UV lamp. The mold produced bar-shaped samples that had identical dimensions, and a hole puncher was used to obtain three circular samples from every bar of cured resin. Fig. 5 illustrates the bar-shaped sample and the smaller, circular sample hole punched from the bar, respectively.

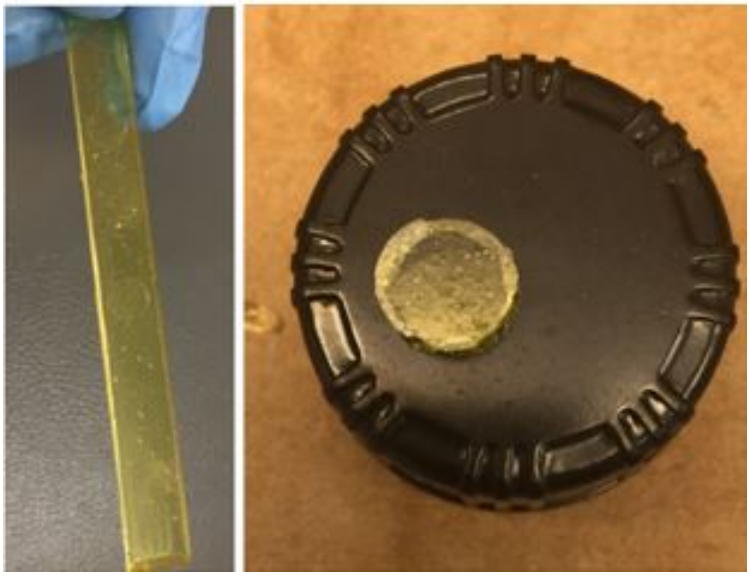

*Figure 5.* Printed samples produced using UV light.

After preparing each sample, each cured resin was compared side by side. Although no physical property testing was performed, it was observed that cured samples containing higher percentages of PEGDA were much more rigid than other samples containing high percentages of PEG. The correlation observed suggests that samples with a high percentage of PEGDA would be capable of withstanding more stress than samples with lower PEGDA percentages.

Kirby-Bauer tests were performed to determine the elution of antibiotics through the cured resin. As predicted, as the percentage of PEGDA increased, elution of antibiotics continued to decrease. The kill study results can be viewed in Fig. 6.

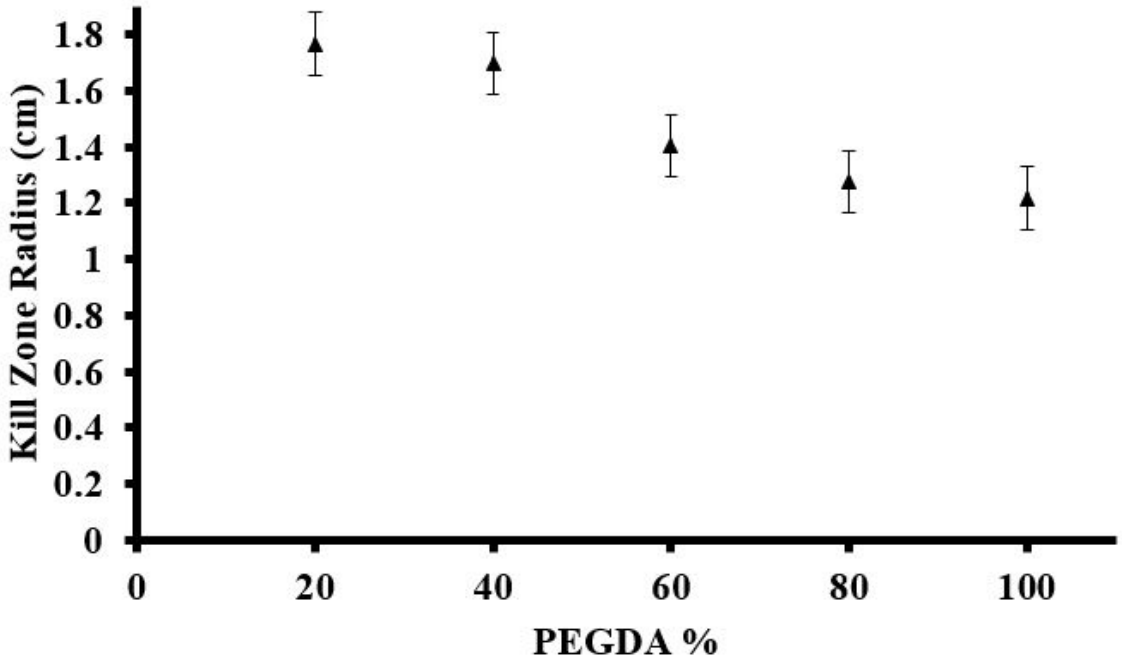


*Figure 6.* Kirby-Bauer test result.

Fig. 6 shows the kill zone radius when changing the percentage of PEGDA from 20 to 100%. The kill zone decreases from 1.8 cm to 1.2 cm highlighting the effectiveness of antibiotics for all PEGDA percentages. After analyzing the raw data, the standard deviation of the data points within each specific composition was calculated. For each composition, three identically sized samples were submitted for kill studies. These kill radii and standard deviation calculations appear in Table 1.

Table 1

*Raw data of SLA kill studies and standard deviation of the data*

| PEGDA (%) | Kill Radius #1 (cm) | Kill Radius #2 (cm) | Kill Radius #3 (cm) | Mean (cm) | Standard Deviation (cm) |
|---|---|---|---|---|---|
| 20 | 1.72 | 1.86 | 1.73 | 1.77 | 0.07 |
| 40 | 1.65 | 1.72 | 1.72 | 1.7 | 0.06 |
| 60 | 1.49 | 1.36 | 1.37 | 1.41 | 0.06 |
| 80 | 1.41 | 1.17 | 1.25 | 1.27 | 0.10 |
| 100 | 0.98 | 1.26 | 1.41 | 1.22 | 0.18 |

In Table 1, it can be observed that for PEGDA volume percentages of 80 and 100 percent, the standard deviation was rather high (0.100 cm and 0.175 cm, respectively) compared to the lower percentages. This uncertainty level may prove that the relationship between PEGDA percentage and kill radius are not linear due to the range of each three-sample study. However, when viewing the raw data visually, the trend of decreasing kill radius with increasing PEGDA appears to hold true, which

allows for confidence when discussing the correlation.

Intuitively, this correlation is understandable, as the increased number of crosslinks would create a stronger network within the cured resin, making it more difficult for a substance to enter or exit the material. For the biocompatible resin, this concept applied to the antibiotics, as they lacked the ability to release freely from the cured sample.

### 2.4 Summary

Exposure to temperature (20 to 230 $^0$C) had little effect on the efficacy of doxycycline, vancomycin and cefazolin. However, UV light did adversely impact vancomycin. In fact, cefazolin did not lose its efficacy, doxycycline lost close to 14.5% and vancomycin about 58%. Thereby, the three antibiotics can be used in the FDM printer but only cefazolin and doxycycline can be in SLA implant. In the next chapter, we will study drug delivery in cubic shaped implant with built-in reservoir experimentally using High Performance Liquid Chromatography (HPLC) and validating the results obtained numerically in COMSOL.

# Chapter 3

# Experimental and Numerical Studies on Drug Elution through 3D Printed Implant With Built-in Reservoir

The purpose of this chapter is to investigate the elution of doxycycline through cubic shaped implant with built-in reservoir. The implant was manufactured using 3D printing FDM technique and the drug elution was studied for a period of 15 days. The concentration of eluted doxycycline was determined via the use of High Performance Liquid Chromatography (HPLC). For the experiment, a mixture of 25 mM of monobasic potassium phosphate buffer and acetonitrile was used as the mobile phase alongside a Discovery column C8 (length 15 cm, inner diameter of 4.6 mm and particle size of $5\mu m$). A retention time of 9.56 min was obtained for doxycycline, consistent with other studies in the literature. Furthermore, doxycycline eluted in a controlled manner and 70 % of the initial amount was eluted after 15 days. A computational model of the implant was generated and the drug elution was determined using COMSOL. Results indicate that the steady-state occurred after 30 days.

## 3.1 Introduction

Drug delivery is a mechanism of delivering pharmaceuticals in humans and animals for a therapeutic purpose. It is typically used for the purpose of controlled release or targeted delivery [37]. The controlled release mechanism serves many functions including prolonged drug release duration [37]. G. Tiwari et al. analyzed the liposomal delivery to increase the efficacy of an anticancer drug [38].

Diffusion is the principal mode through which drug is delivered in a variety of applications [39]. Diffusion is the transport phenomena of molecules from one medium to another due to random molecule motion. Drug diffusion takes place in

two main systems: reservoir and monolithic system. In the reservoir system, drugs diffuse through a polymeric membrane to reach to the outside environment. In the monolithic system, the drug is mixed with the polymer. Therefore, the diffusion happens with an initial burst of release which implies the drug release phenomena [37, 40].

The application of drug delivery in medical application has been studied by several authors [41, 42]. These include implantable microfluidic device for neurological disorders delivering drug directly into brain tissue, a magnetically activated drug delivery implant via reservoir system as well as periprosthetic implants for orthopedic applications [32, 41, 42].

In this chapter, we propose examining the elution of doxycycline Poly-lactic acid (PLA) implant using the reservoir system. This will be done by 3D printing an implant with reservoir where the doxycycline solution will be injected. The implant will be submerged in 40 mL of 0.9% sodium chloride irrigation, also called saline. High Performance Liquid Chromatography will be employed for detection of released antibiotics.

The retention time of doxycycline will be validated with the findings from studies done by Monser et al., Fiori et al., Shariati et al., and Sigma Aldrich [43-46]. A numerical model to predict drug delivery will be setup in COMSOL and will be calibrated using the experimental data.

### 3.2 Mathematical Background

Diffusion is the principal mode through which drug is delivered and the rate of diffusion is proportional to the diffusion coefficient, time and concentration. The general form of the diffusion-convection equation is used to predict the concentration

$(c(x,t) \approx c)$ in anisotropic and heterogeneous media as given below [47]:

$$\frac{\partial c}{\partial t} + \frac{\partial c u_j}{\partial x_j} = \frac{\partial}{\partial x_j}\left(D_{ij}\frac{\partial c}{\partial x_j}\right) + R \tag{1a}$$

Initial Condition:

$$c(x,0) = c_0 \tag{1b}$$

Dirichlet Boundary Condition:

$$c(x) = c_d(\forall x \in \partial B) \tag{1c}$$

Neumann Boundary Condition:

$$-n_i D_{ij}\frac{\partial c}{\partial x_j} + n_j u_j c = J_n(\forall x \in \partial B) \tag{1d}$$

Where $\mathbf{u}$ is the velocity, $R$ is the source, $t$ is time, $\mathbf{x}$ is position, $D_{ij}$ is the anisotropic diffusivity, $c_0$ is the initial concentration of the antibiotics at $t = 0$, $c_d$ is the concentration of antibiotics at the boundary B, $\mathbf{n}$ is the normal vector and $J_n$ is the normal flux. In special case when $\mathbf{u}$ is zero and $R$ is zero, use of Eq. 1a results in Fick's second law:

$$\frac{\partial c}{\partial t} = \frac{\partial}{\partial x_i}\left(D_{ij}\frac{\partial c}{\partial x_j}\right) \tag{2}$$

For the steady-state situation, Eq. 2 takes the following form:

$$\frac{\partial}{\partial x_i}\left(D_{ij}\frac{\partial c}{\partial x_j}\right) = 0 \tag{3}$$

The diffusivity $\mathbf{D}$ is in general second-order anisotropic tensor given as follows:

$$\mathbf{D} = \begin{pmatrix} D_{ii} & D_{ij} & D_{ik} \\ D_{ji} & D_{jj} & D_{jk} \\ D_{ki} & D_{kj} & D_{kk} \end{pmatrix} \tag{4}$$

When viewed in the principal direction, the diffusivity takes the following form:

$$\mathbf{D} = \begin{pmatrix} D_i & 0 & 0 \\ 0 & D_j & 0 \\ 0 & 0 & D_k \end{pmatrix} \tag{5}$$

Where $D_i$, $D_j$ and $D_k$ are the principal diffusivities. For the special case of isotropic media, Eq. 4 takes the following form

$$\mathbf{D} = D \begin{pmatrix} 1 & 0 & 0 \\ 0 & 1 & 0 \\ 0 & 0 & 1 \end{pmatrix} \tag{6}$$

Finally, for axisymmetric problem, the Fick's second law (Eq. 2) takes the following form [48]:

$$\frac{\partial c}{\partial t} = \nabla.(\mathbf{D}\nabla c) = \left[\frac{1}{r} D_r \frac{\partial}{\partial r}\left(r \frac{\partial c}{\partial r}\right) + D_z \frac{\partial^2 c}{\partial z^2}\right] \tag{7}$$

### 3.3 Materials

Doxycycline hyclate (or also called doxycycline hydrochloride hemiethanolate hemihydrate) was obtained from Sigma-Aldrich shipped from Milwaukee. Its empirical formula is $C_2 2H_2 4N_2O_8.HCl.0.5H_2O.0.5C_2H_6O$ , its molecular weight is $M = 512.94 g/mol$ and the maximum solubility in water is $50 mg/mL$. Fig. 7 shows the chemical structure of doxycycline hyclate.

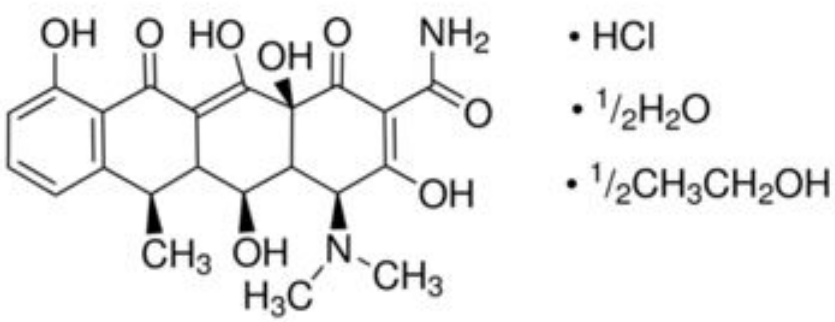


*Figure 7.* Chemical structure of doxycycline hyclate from Sigma Aldrich.

The 3D printer used is Ultimaker 2+ from the Ultimaker Company. For PLA, it was preferable to order natural PLA from Sigma Aldrich with diameter 2.85 mm. The natural PLA used has a density of 1.25 g/cm$^3$ [49].

### 3.4 Experimental Setup

**3.4.1 Stages in 3D printing of the implant**. A CAD model of the implant was created in SOLIDWORKS. The outside dimension of the cubic implant was $0.94in \times 0.94in \times 0.26in$ and the dimension of reservoir was $0.79in \times 0.79in \times 0.1in$. Fig. 8 shows the 3D printed cuboid implant.

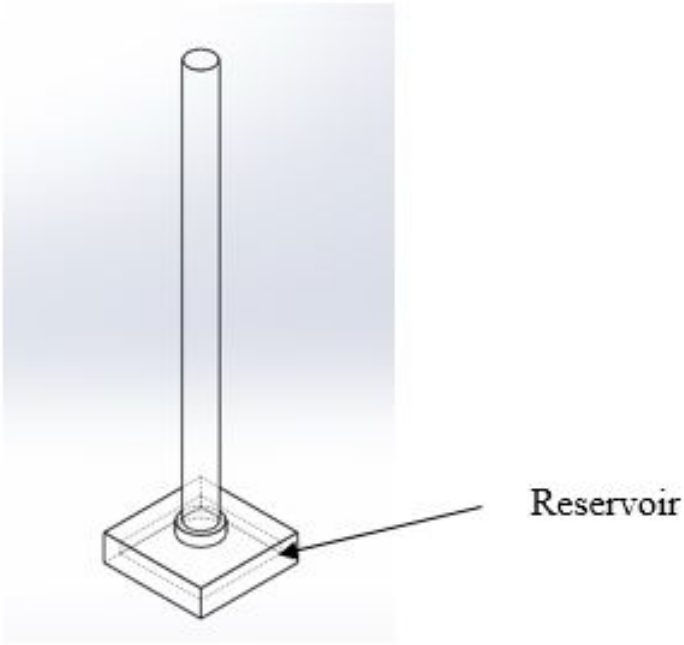


*Figure 8.* Cuboid implant.

The microstructure of the printed part is significantly affected by the print settings. Some of these settings include infill percentage, print orientation, temperature of build plate and nozzle, speed of printing and material flow among others. This could have significant impact in the drug delivery. In this study, the nozzle diameter was set to $0.4mm$, layer height was $0.1mm$, wall thickness was $1.05mm$ but the top and bottom thickness were $0.8mm$. The infill density was set at 20% and the speed of printer head was $50mm/s$. Finally, the support structure was only used in the build plate.

**3.4.2 Design of experiment**. The implant was merged into 40 mL of saline (0.9% sodium chloride irrigation, USP). Doxycycline Hyclate with concentration of 10 mg/mL was injected into the reservoir by pausing the printer during the print stage. Fig. 9 shows the experimental setup used in the study.

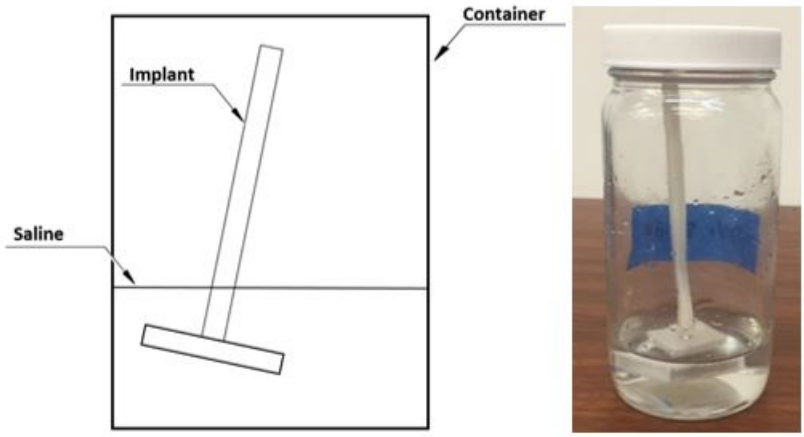


*Figure 9.* Experimental setup of the cuboid implant.

### 3.5 HPLC Experiment

**3.5.1 Material used**. Monobasic potassium phosphate (Worldwide Life Science, Bristol, PA) mixed with 1L of Deionized water and HPLC Acetonitrile Acs, Reagent and pH (EMD Millipore, Billerica, MA) were the reagents used for HPLC experiment. The monobasic potassium phosphate buffer was prepared by mixing

3.41g of the salt in 1L of deionized water to create the buffer with molar concentration of 25 mM. The two mobile phases were prepared and suggested following Sigma Aldrich technical paper.

**3.5.2 HPLC methodology**. The detection and determination of the solutions were done using HPLC Agilent 1100. The system consists of JetDirect card connected to the detector, G1310A isocratic pump with solvent container, G1314A VW detector with flow cell and G1328A Manual Injector, PC, monitor and software for post-processing the data obtained. The Column used is SUPELCO Discovery column C8 (length 15 cm, inner diameter of 4.6 mm and particle size of 5 $\mu$m). The mobile phase flow rate was 1 mL/min. The detection wavelength was set to 260 nm and the injection volume was set to be 55 $\mu$L. Fig. 10 shows the gradient used for the mobile phase. Based on published data by Sigma-Aldrich, detection of doxycycline was expected to be within 15 minutes. The second phase was run for 5 minutes to clean the HPLC from any elements leftover. The third phase was used to prepare for the next experiment.

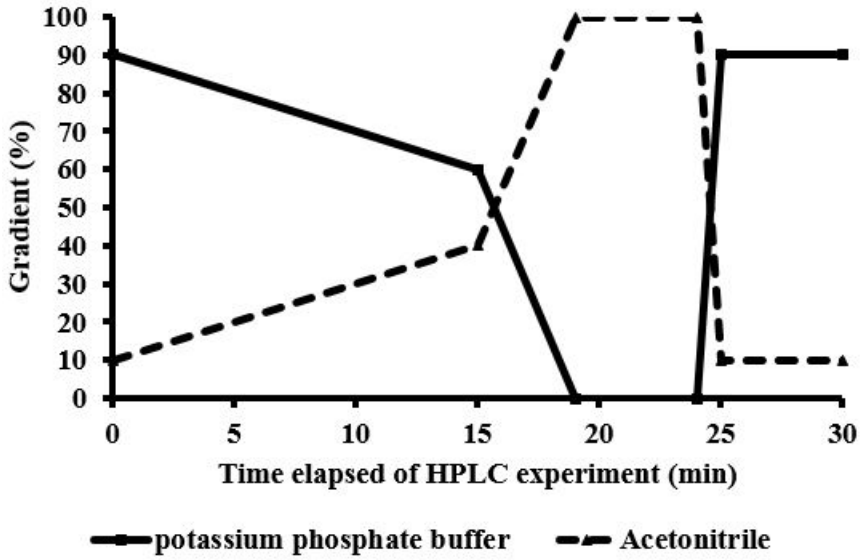


*Figure 10.* Mobile phase methodology.

**3.5.3 Calibration curve**. The chromatogram resulted gives the absorbance values, using which concentration can be inferred. In this thesis, the antibiotics considered were in the range of 0.1-0.5 mg/mL with an increment of 0.05 mg/mL. Fig. 11 shows the baseline curve of concentration versus absorbance as obtained using HPLC. Clearly, the results indicate that the concentration increases with increasing absorbance values, albeit in nonlinear manner.

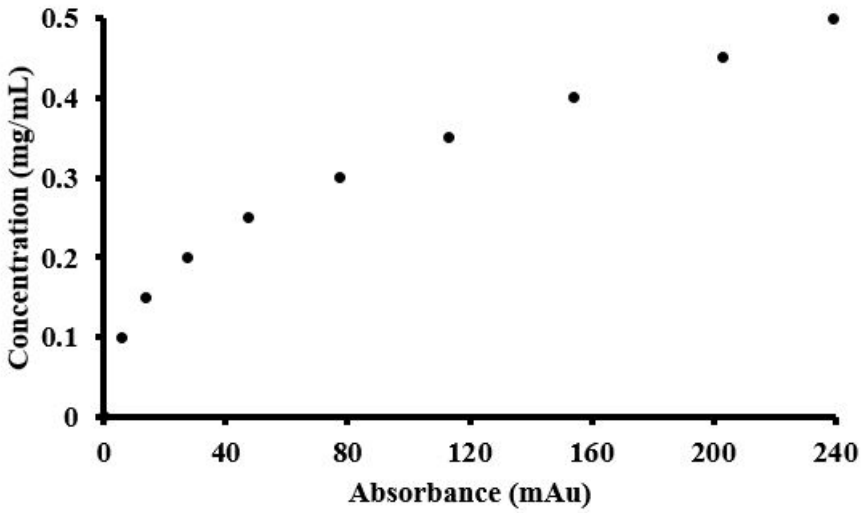


*Figure 11.* Baseline curve of HPLC experiment.

### 3.6 COMSOL Experiment

**3.6.1 Geometry, initial and boundary conditions**. The axisymmetrical model (symmetry about the vertical axis) of the implant (see Fig. 9) and the surrounding saline solution is shown in fig. 12. The inner domain is the reservoir containing the antibiotics which held within the PLA implant. The volume of the saline is 2.44 $in^3$, the radius of the beaker is 1.19 in and the height is 0.55 in. The PLA domain dimension in COMSOL is 0.47 in $\times$ 0.26 in and the reservoir domain has a dimension of 0.395 in $\times$ 0.1 in.

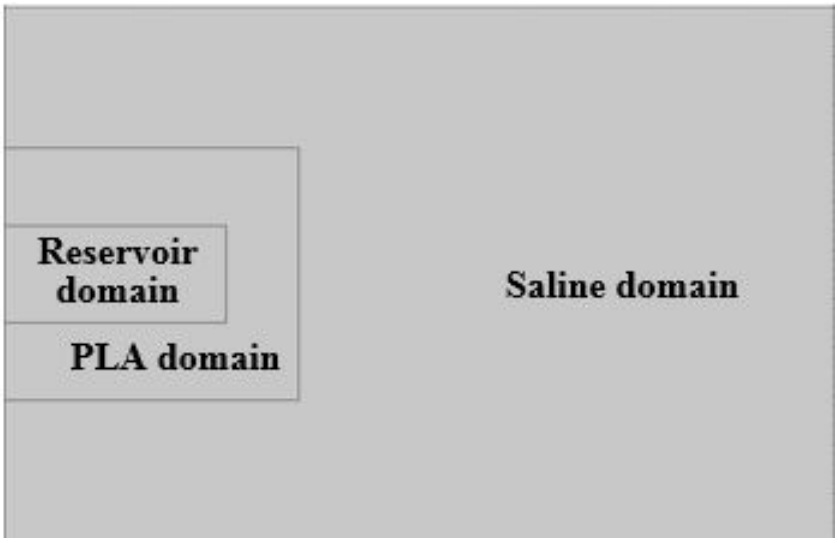


*Figure 12.* The geometry created in COMSOL.

In this study, saline ($D_s = 1.99 \times 10^{-9} m^2/s$) and doxycycline solution ($D_d = 1.2 \times 10^{-11} m^2/s$) are considered to be isotropic but PLA is considered anisotropic due to the directionality in the 3D printing process [50] with the following second rank diffusivity tensor:

$$D_p = \begin{bmatrix} 2.917 \times 10^{-13} & 0 \\ 0 & 9.147 \times 10^{-12} \end{bmatrix} m^2/s \tag{8}$$

The initial condition is the initial concentration ($c_i$) of the antibiotic solution in each domain. Since the solution only exist in reservoir domain, $c_i$ is zero in PLA and saline domain but within the reservoir, the initial concentration is 10 mg/mL $\approx$ 19.5 mol/$m^3$ . As for boundary condition, there is no flux at the outside boundary because of no loss and no boundary at the axisymmetric axis.

**3.6.2 Mesh generation**. Selecting appropriate mesh size is extremely important for accuracy when solving initial boundary value problems using finite element analysis. The size, shape, number of elements and time step are among the parameters that need to be tuned. In COMSOL, when using either 2D or 2D axisymmetric geometry, there are different ways of generating a mesh such as the default way focuses on the number of elements. Usually, in this case, higher elements lead to better results, but at the cost of a longer computation time. Changing the shape of meshing is also an option by either choosing tetrahedral, quadrilateral, triangular or mapped elements. Table 2 compares the settings for each meshing types.

Table 2

*Comparison between the six meshes settings*

| Mesh Type | Mesh's information | | | | | | |
|---|---|---|---|---|---|---|---|
| | Time Step | Number of elements | Run time (s) | Reciprocal error at initial time step | Reciprocal error at final time step | $c_{max}$ (mol/ $m^3$) | $c_{min}$ (mol/ $m^3$) |
| Mapped/free triangular - Extremely Fine | 40 | 6240 | 4 | 0.01695 | 8.27e-6 | 1.33 | 0.36 |
| Mapped and free traingular - Finer & 0.0796 in | 48 | 2252 | 4 | 0.0254 | 3.416e-6 | 1.35 | 0.36 |
| Free Triangular - Extra Fine | 37 | 1610 | 2 | 0.0076 | 8.27e-6 | 1.31 | 0.36 |
| Controlled Mesh 1- Extra Fine | 37 | 1610 | 2 | 0.0076 | 8.27e-6 | 1.31 | 0.36 |
| Controlled Mesh 2 - Finer | 34 | 516 | 1 | 0.00485 | 9.45e-6 | 1.24 | 0.35 |
| Free Quad and triangular -Extremely Fine | 38 | 5926 | 4 | 0.0161 | 8.26e-7 | 1.3 | 0.36 |

Due to the higher number elements, smaller initial reciprocal error and adequate time step, we choose the extremely fine section of mapped/free triangular. Fig. 13 shows the convergence and meshing for the computational model.

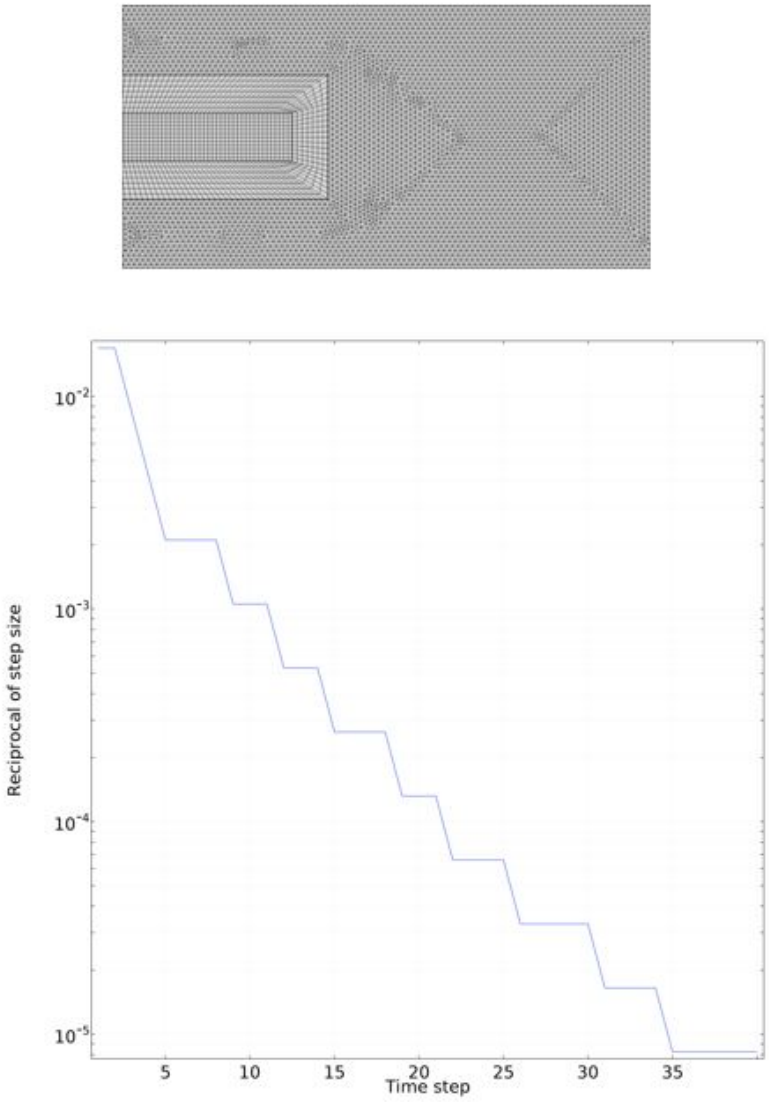


*Figure 13.* Mapped and free triangular mesh with 6240 elements. The X and Y-axis represents the dimension of the geometry created, the convergence shows the error Vs time step.

### 3.7 Results and Discussions

A total of five experiments (see Appendix A) were conducted on doxycycline solution using HPLC Agilent 1100 to detect the retention time [46]. Fig. 14A shows chromatogram of five antibiotics under the family of tetracycline detected by Sigma Aldrich and Fig. 14B shows the retention time.

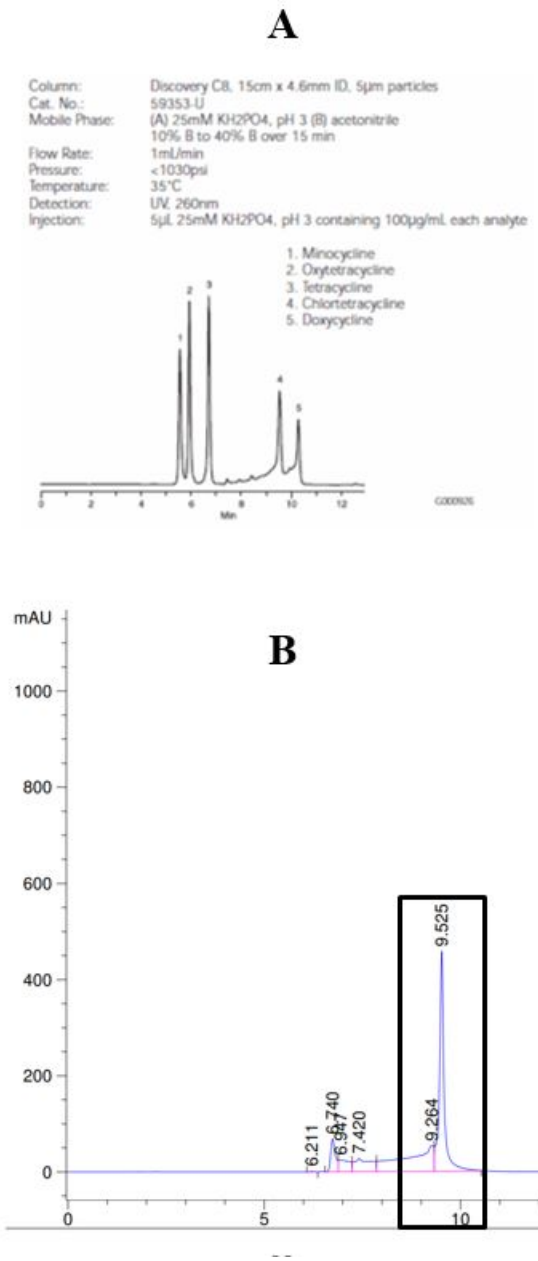


*Figure 14.* Comparison of results between Sigma-Aldrich methodology [46] and one of the chromatography from current work. A) The proposed B) Sigma Aldrich methodology. The Y-axis represents the absorbance, X-axis represents retention time.

The retention time of doxycycline based on the current work is 9.59 ± 0.06 minutes and compare well with the results from Sigma Aldrich (10 minutes). The slight difference in retention time could be attributed to factors such as different HPLC devices and mobile phase (see Table 4). Additionally, there has been an increase of acetonitrile from 40% to 100% in order to clean the noise and be able to run the experiment again. Lastly, Sigma Aldrich analyzed a sample made of doxycycline mixed with the monobasic potassium phosphate buffer $KH_2PO_4$ whereas in the present study, saline was used in the solution [51].

Table 3

*The comparison between Sigma Aldrich methodology and the current work in HPLC experiment [46]*

| **HPLC's parameters** | **Sigma Aldrich methodology A** | **Current Work** |
|---|---|---|
| **HPLC machine** | Water Alliances 2487 | Agilent 1100 |
| **Injection** | 5 $\mu$L | 5 $\mu$L |
| **Column** | Supelco Discovery C8 (15 cm × 4.6mm ID, 5 $\mu$m particles) | Supelco Discovery C8 (15 cm × 4.6 mm ID, 5 $\mu$m particles) |
| **Mobile phase** | (A) 25 mM $KH_2PO_4$,pH 3, (B) Acetonitrile 10 % B to 40 % B over 15 minutes | (A) 25 mM $KH_2PO_4$, pH 3.4, (B) Acetonitrile 10 % B to 40 % B over 15 minutes, 100 % B over 5 minutes |
| **Flow Rate** | 1 mL/min | 1 mL/min |
| **Temperature** | 35 $^0$ C | |
| **Pressure** | < 70.1 atm (1030 psi) | < 100 atm (1469.59 psi) |
| **Detection** | UV, 260 nm | UV, 260 nm |

The use of reversed phase HPLC on doxycycline have been widely studied for different purpose. Monser et al. proposed running HPLC experiment on five tetracycline families to separate them from the pharmaceutical product. The HPLC used is called Beckman HPLC characterized by HPLC device equipped with UV 166 variable wavelength spectrophotometer. The column used is carbon column filled with hypercab porous graphitic carbon with dimension 10 cm $\times$ 4.6 mm I.D.,7 $\mu$m of particle size. The mobile phase used is a mixture of potassium dihydrogenophosphate buffer 50 mM,pH 2 and 40% of volume-to-volume of acetonitrile run for a period of 15 minutes. The flow rate of the mobile phase is 1 mL/min and the injection of the sample is 20 $\mu$L. The resulted retention time is 11.2 min [43].

Fiori et al. used HPLC to detect doxycycline mixed with acid water and acetonitrile. The HPLC used is Hewlett Packard, also called HP, Ti Series 1050 liquid chromatography equipped with Rheodyne 7125 injector. The chosen column is Phenomenex Luna C18 with dimension of 15 cm $\times$ 2.0 mm I.D. with particle size of 3.5 $\mu$m. The mobile phase is a mixture of oxalic acid (0.02 M,pH 2.5), acetonitrile and methanol with volume ratio of 75-17-8. Doxycycline was detected around 12 minutes [44].

Shiariati et al. used HPLC to extract tetracycline, oxytetracycline and doxycycline in bovine milk, human plasma and water samples. The authors use Varian 9012 HPLC alongside Varian 9050 wavelength UV/Vis for detecting the antibiotics in the solution. 20 $\mu$L of the sample were manually injected using Rheodyne 7725 injector. The column used is Supelco C18 analytical with dimension 15 cm $\times$ 4.6 mm I.D.,3 $\mu$m of particle size). The mobile phase is a mixture of oxalic acid (0.005 M, pH 2.4), methanol and acetonitrile with volume ratio of 71:16:31 volume-to-volume-to-volume in the first 6 minutes and ratio of 50:25:25 volume-to-volume-to-volume between 6 and 15 minutes. The flow rate and the

detection wavelength were respectfully 1 mL/min and 360 nm. The retention time of doxycycline is 10 minutes [45].

Fig. 15 compares the result of Sigma Aldrich, Fiori, Monser, Shariati and the current work. Even though different columns with same inside diameter and different methodologies were employed, the retention times were closer to each other. In fact, the margin difference was very small. Therefore, when using a carbon column type with dimension 10-15 cm × 2-4.6 mm ID, the retention time of doxycycline ranged between 9.5 and 12 minutes.

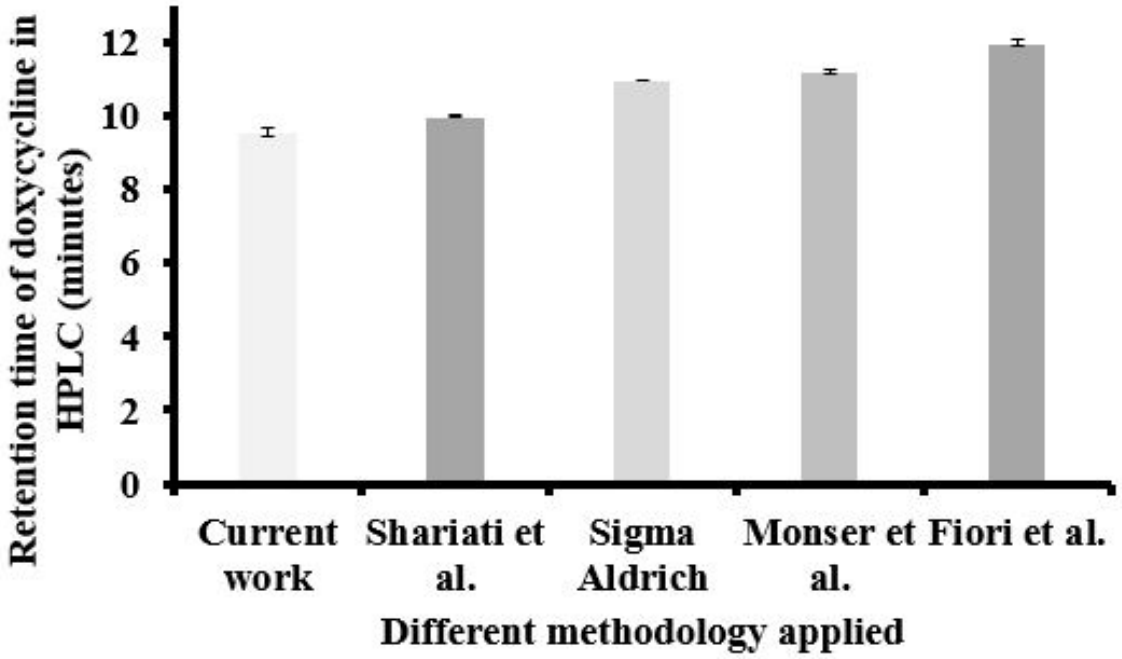


*Figure 15.* The comparison of retention time between different methodologies.

Fig. 16 represent the experimental versus numerical results during a period of 2 weeks. The experimental result shows a drug elution increasing in controlled manner. However, it did not reach steady-state level within this time period. Overall, there is a good match between computational and experimental results (maximum error of 10%).

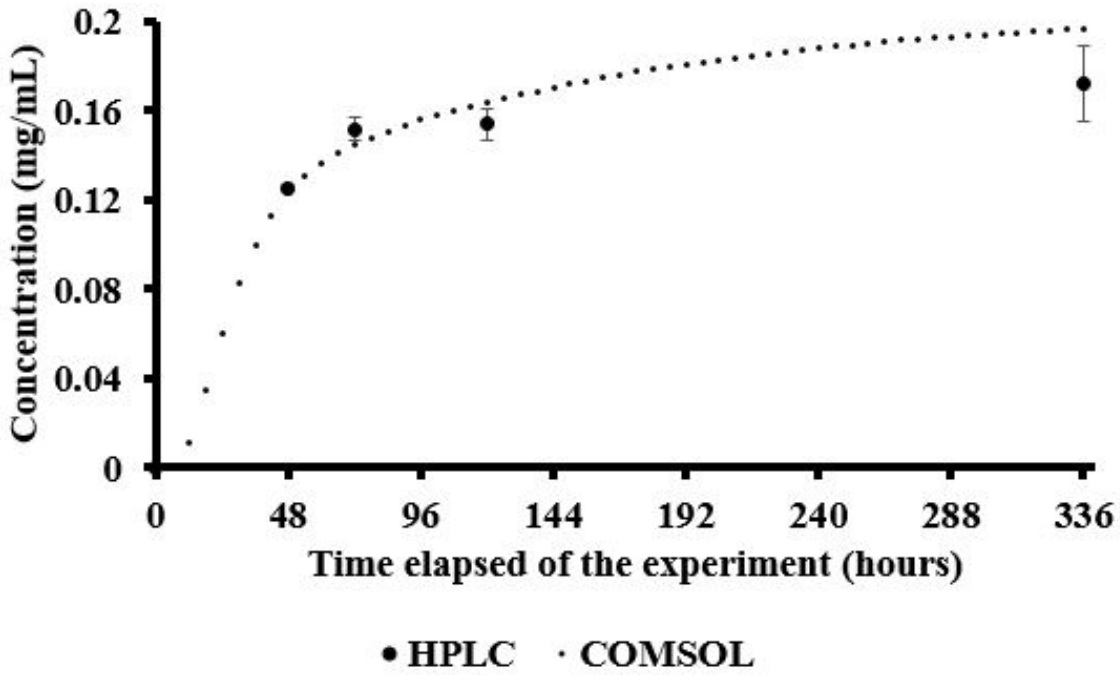


*Figure 16.* Comparison between Experimental and COMSOL results at different time.

Fig. 17 shows the percentage release of doxycycline from the 3D printed implant using HPLC and COMSOL data. The percentage release was computed by first calculating the initial and final amount. The initial amount is 10 mg since m=$c_i$ × V=10 mg/mL × 1 mL=10 mg, and the final amount is the product of the final concentration and the total volume of the saline (40 mL). Dividing the final amount to the initial amount yields the percentage release. For a period of 14 days, there is a total release of over 70% of initial amount of doxycycline.

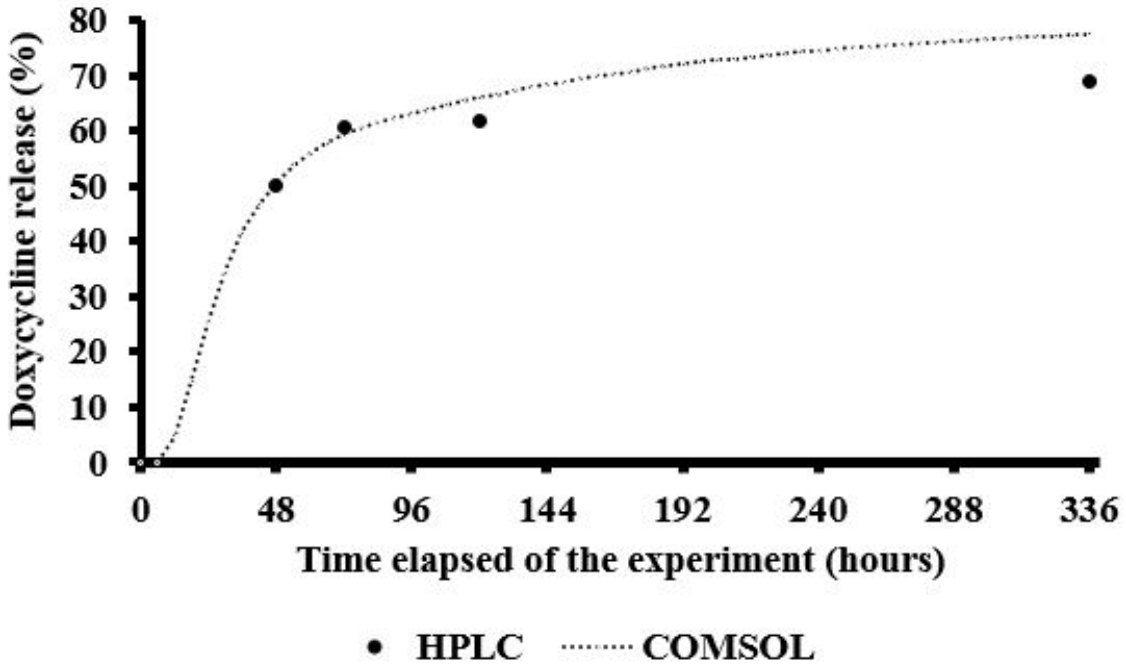


*Figure 17.* The comparison between the HPLC and COMSOL results in percentage release.

Fig. 18 shows the contour plots of the experimental setup at time 0, 24, 48, 72, 120 and 336 hours. In the first day, 7 mol/$m^3$ of concentration eluted from the reservoir indicating a release of 36%. By 48 hours, more than 50% was eluted. Based on these results, the half-time period for the elution of doxycycline through this PLA implant is estimated to be about 47.02 hours (about 2 days). Even though the saline domain does not change color, the legend shows an increase of concentration. At zero hours, the minimum concentration was negligible. At 336 hours, the minimum concentration was 0.375 mol/$m^3$ indicating a total elution over 70 %.

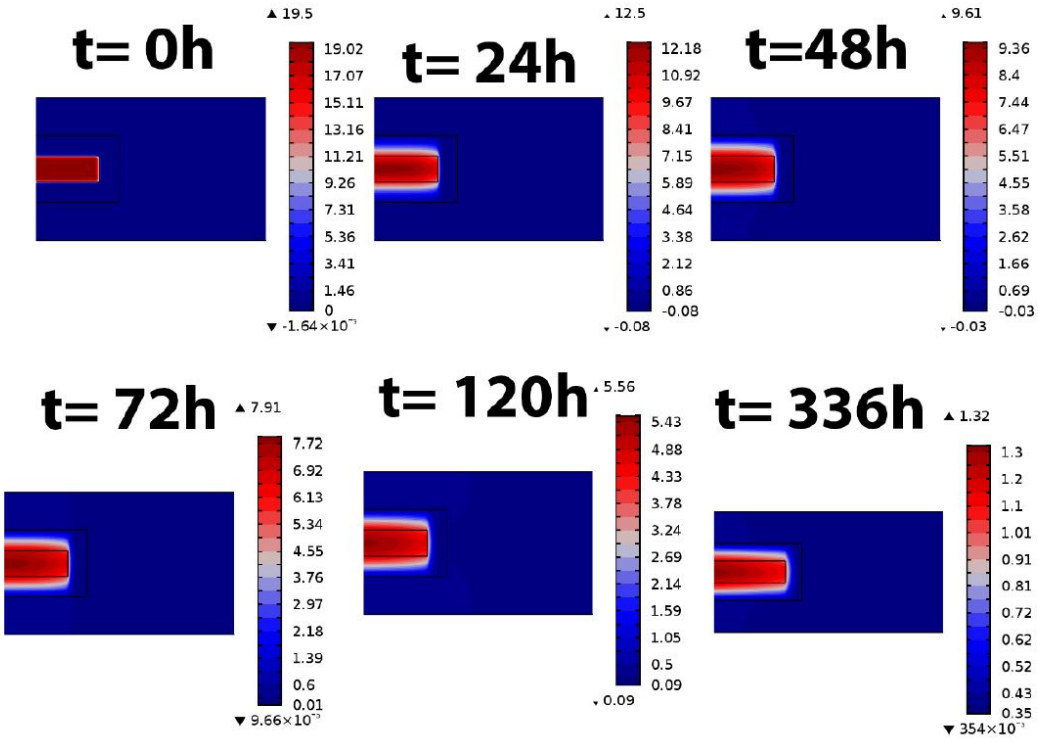


*Figure 18.* Contour plot of the numerical simulation at different time period. The number at the end of the legends are considered to be equal to zero.

Fig. 19 shows the change of concentration in r-direction. At the boundaries, there is no release of antibiotics when time is equal to zero hours since the diffusion did not start yet. As for 336 h, the concentration gradient is almost negligible (a decrease of 0.02 mol/$m^3$). The change of concentration slope increased in the first two days but start decreasing from the third day due to passing half-time period of elution. The graph at the right side shows the concentration gradient from reservoir to the outside domain. Before reaching PLA surface, the concentration is steady to the change of r-direction until it reaches PLA surface. At the boundary, the concentration exponentially decreases until it becomes negligible then increases with small increment when leaving into saline domain due to the non-homogeneous boundary between PLA surface and reservoir domain. This phenomena explains the concentration in the PLA surface shown in Fig. 19.

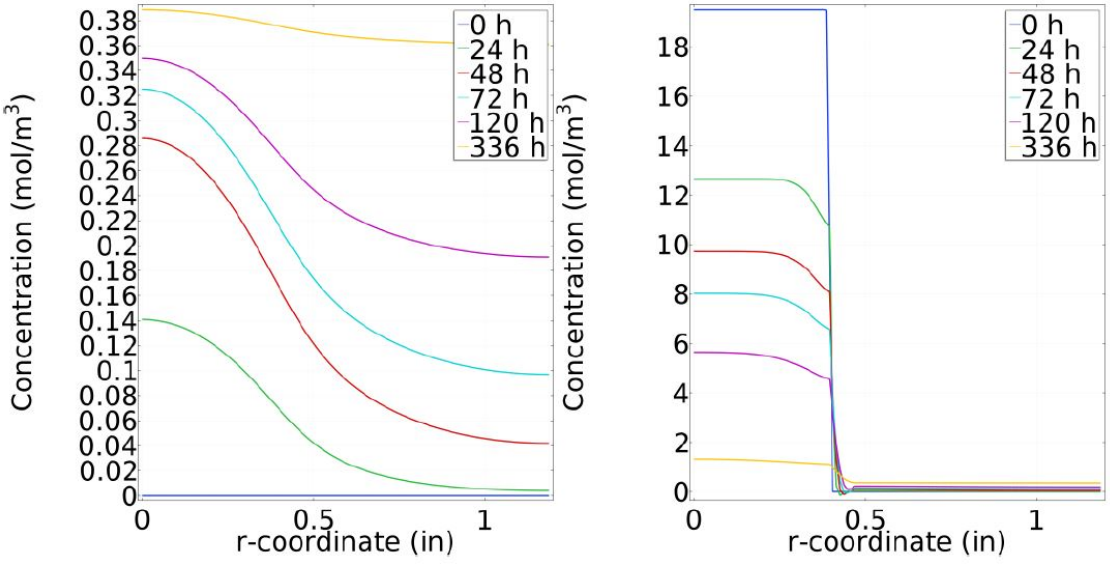


*Figure 19.* The change of concentration along r-direction: The left plot represents at the boundaries, the right represents from the reservoir to saline domain.

Fig. 20 shows the flux from reservoir to saline domain. The total flux defines the transfer rate. According to Fick's first law, flux is dependent on the concentration gradient and the diffusion coefficient. In this case, the diffusion coefficient is fixed for each domain. However, the concentration gradient changes because of the release. Since there is a big drop in concentration gradient at the surface PLA as shown in Fig. 19. This explains the flux peak closer to the PLA surface. The diffusion coefficient being very low implies the negligibility of total flux. The fluxes are higher at the boundary between PLA surface and reservoir and between PLA surface and saline. This could be explained due to the diffusion coefficient of each domain.

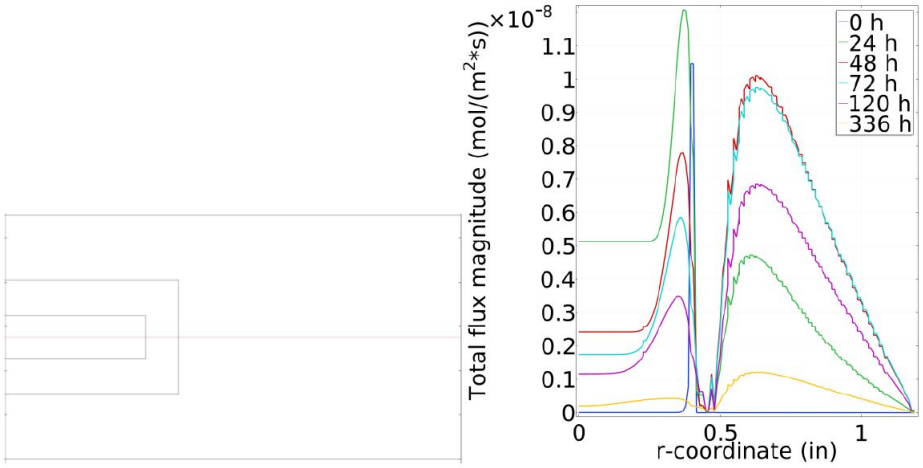


*Figure 20.* Total flux from reservoir to saline.

Fig. 21 compares the concentration versus time at three different points when the elution reaches steady-state level. The blue graph shows the COMSOL result that was compared to the experimental result which is closer to the reservoir domain. The green graph shows the concentration at the end of the PLA surface and the red graph shows the concentration at the end of saline domain. As a result, the farther we are from the reservoir, the lower the antibiotic elution rate. On the other hand, the three curves reach steady-state level at 700 hours (closer to 1 month) and the steady-state concentration of the three graphs are all equal to 0.3902 mol/$m^3$ $\approx$ 0.200 mg/mL. The amount of doxycycline eluted from the reservoir at steady-state: 0.200mg/mL $\times$ 40 mL=8 mg since the saline domain has a volume of 40 mL. The initial amount inside of the reservoir is 10 mg: 10 mg/mL $\times$ 1 mL=10 mg. Therefore, this analytical calculation validates the accuracy of the concentration in steady-state. Moreover, according to our numerical result, 80% of the amount of doxycycline will elute by 700 hours. The 20% will be left in the PLA surface since the elution reaching steady-state implying that there is no more antibiotic in the reservoir.

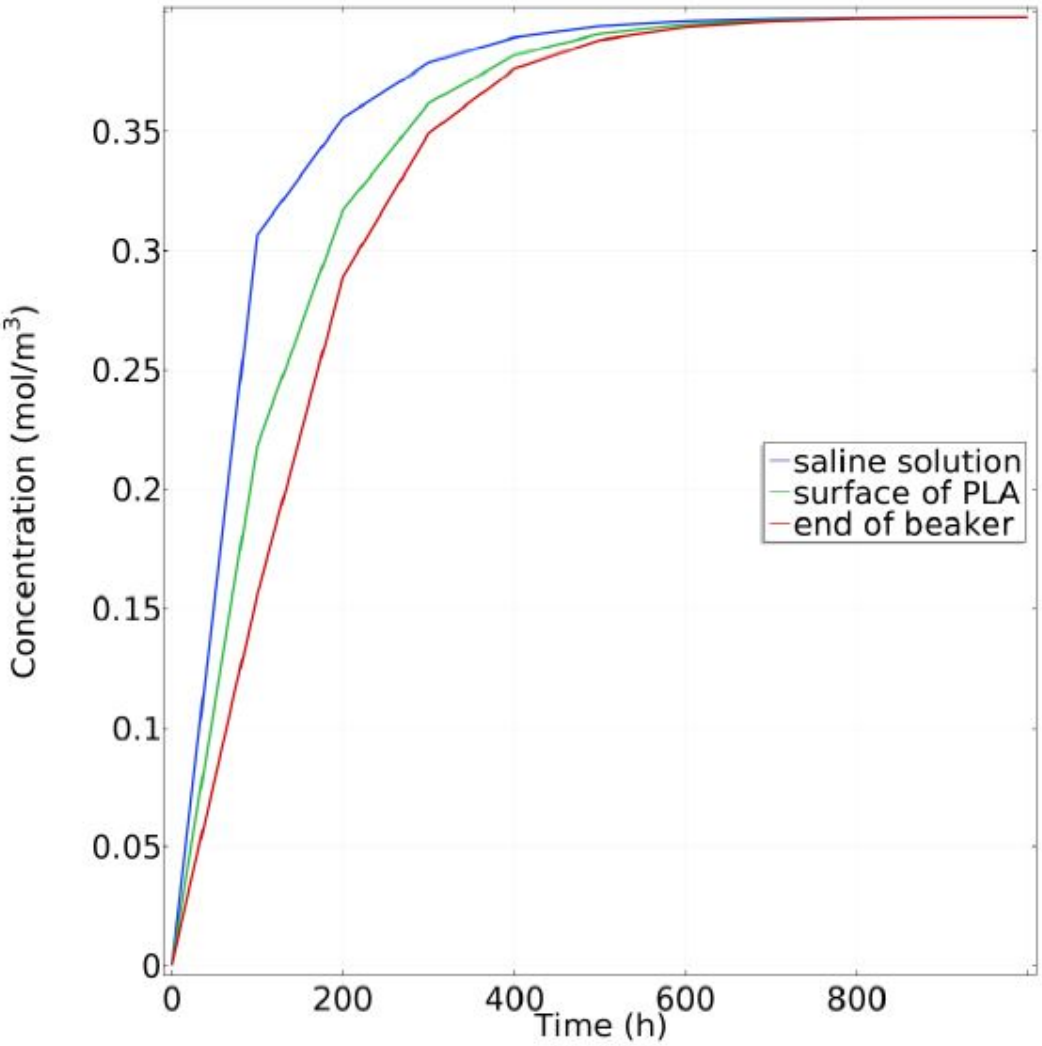


*Figure 21.* Comparison of the eluted concentration at different time.

### 3.8 Summary

The drug elution in an implant with reservoir features has proven to be efficient. For a period of 15 days, about 70% of doxycycline was released. Quantifying the amount eluted was done through HPLC. Using carbon-based column and mobile

phase made of mixture between buffer and organic solution, the retention time of doxycycline was found around 9.56 min.

The experimental study was a validation to numerical simulation. The concentration contour, gradient and change of flux were examined for optimization. The half-time of the drug elution is 47 hours. Additionally, it was numerically predicted that the elution will stabilize after 30 days. By that time, 80% of the amount was released and 20% stayed inside of the surface. Therefore, we propose to investigate drug elution through other polymeric and metal 3D printed hollow shaped orthopaedic implants to better understand the drug elution.

# Chapter 4

## Kill Studies on Antibiotics Eluted through 3D Printed Implants

The purpose of this chapter is to study the elution of doxycycline through 3D printed orthopaedic shaped implant with reservoir and microchannel features using three different materials: Poly-Lactic Acid (PLA), Poly-Caprolactone (PCL) and Titanium grade Ti-6Al-4V. The PLA and Ti-6Al-4V experiments were run for a period of 31 days and the PCL experiment for one day. The antibacterial ability of eluted doxycycline from PCL, PLA and Titanium were inspected using Kirby-Bauer test on the bacteria E.coli k-12. The results show that most of doxycycline eluted through the three materials in the first 24 hours and reached the steady-state level after 30 days for PLA and Titanium. Additionally, Titanium implants released more amount of antibiotics than PLA implant did. The eluted antibiotics through all the implants demonstrated the ability to kill bacteria in the subsequent Kirby-Bauer test. These outcomes prove that 3D printed polymeric and metallic implants with built-in reservoir(s) and microchannel(s) have great potential in orthopaedic applications.

### 4.1 Introduction

Orthopaedic implants are commonly made using metallic alloys (iron, cobalt and titanium) and polymers. Steel based orthopaedic implants are usually made up of 316L stainless steel and iron-based alloy with mixture of iron, chromium, nickel, and small amount of manganese, carbon, molybdenum and silicon. The extra low interstitial (ELI) grade of titanium based of titanium, aluminum and vanadium form the family of titanium implants. Along similar lines, several polymers(ultrahigh molecular weight polyethylene, poly methyl methacrylate, silicone rubber) have been used in articulating joints and bone cement [52]. The focus of this thesis will be on Poly-caprolactone (PCL), Poly-lactic Acid (PLA) and titanium implants.

PCL is a biodegradable, bioresorbable polymer with a melting point of $60^0C$. Woodruff et al. studied the application of PCL in the biomedical field. PCL is suitable for controlled drug delivery due to its high permeability to many drugs and its ability to be fully excreted from the body once bioresorbed [53].

Contrary to PCL, PLA is a thermoplastic material discovered in 1932 by Carothers at DuPont by heating lactic acid under vacuum while removing the condensed water. It is bioplastic and biodegradable material. This thermoplastic is characterized by having glass transition temperature 40 $^0C$- $70^0C$, melting temperature $130^0C$- $180^0C$, a density of 1.25 g/$cm^3$ and tensile strength of 53 MPa. PLA can be applied in food, bone fixation, drug delivery and tissue engineering [49, 54].

Titanium is a metallic element with the atomic number equal to 22. It is characterized by silver color and is the seventh most existed metal in the planet [55]. In medicine, titanium is usually used to create implants for orthopaedic purpose such as plates, screw, or for cardiovascular such as pacemaker [56]. There are many different titanium alloys including Ti-6Al-7Nb or Ti-5Al-3Mo-4Zr. The most used alloy in medical application are Ti-6Al-4V and cpTi. Ti-6Al-4V was originally created for aerospace applications [57]. It has a mechanical properties between 1 and 1.45 GPa and elongation ranging from 25% to 4.4%, and has a mixture of 90% of total weight for titanium, 6% for aluminum, 4% for vanadium, 0.25% of iron and 0.2% of oxygen. It is characterized by a density of 4.43 g/$cm^3$, elastic modulus of 113.8 GPa and ultimate tensile strength of 950 MPa. The melting temperature of Ti-6Al-4V is between 1604 $^0C$ and 1660 $^0C$ [58]. Titanium implants have been widely used for mechanical purpose. However, to the best of our knowledge, there is limited studies of drug delivery through these implants.

The study of antibiotic controlled release through metals has been pursued

by several authors. Adams et al. proposed an in-vivo and in-vitro study by creating vancomycin-containing sol-gel film on Titanium alloy rod (Ti-6Al-4v) to treat infection. The in-vitro study was done in S.aureus culture by implantation of the model into the infected femora. Vancomycin eluted in five days in the in-vitro study and the 28 days in in-vivo study implying an elution in controlled manner [59].

This chapter will study the elution of doxycycline from PCL, PLA and Ti-6Al-4V 3D printed implant with built-in features such as reservoir and microchannel for a period of 31 days, for PLA and Titanium, and 24 hours for PCL mixed with antibiotic. The success of the eluted doxycycline regarding antibacterial ability will be tested using Kirby-Bauer test on the bacteria E. coli k-12 strain. The Minimum Inhibitory Concentration (MIC) of doxycycline will be used for baseline studies.

Kirby-Bauer test has been extensively used for antibacterial susceptibility studies. Neut et al. explored the potential creation of antimicrobial when combining fusidic acid or clindamycin with gentamycin loaded in bone cement using Kirby-Bauer test [60]. Rossi et al. used Kirby-Bauer test to determine the minimum inhibitory concentration of Gentamicin on the bacteria Staphylococceus Aureus and haemolyticus [61]. Andrews explores the determination of minimum inhibitory concentration for different antibiotics using E. coli k-12 instead. The minimum inhibitory concentration of Tetracycline in E. coli is 0.002 mg/mL [62].

## 4.2 Material and Methodology

**4.2.1 Materials**. The antibiotic used is doxycycline monohydrate ($M_w$=462.45 g/mol) . It is soluble in ethanol or methanol but barely in water. The antibiotic was obtained from World Wide Life Science, Bristol PA (from vendor Alfa Aesar). The chemical formula for doxycycline monohydrate is $C_22H_24N_2O_8.H_2O$ and the chemical structure is shown in Fig. 22.

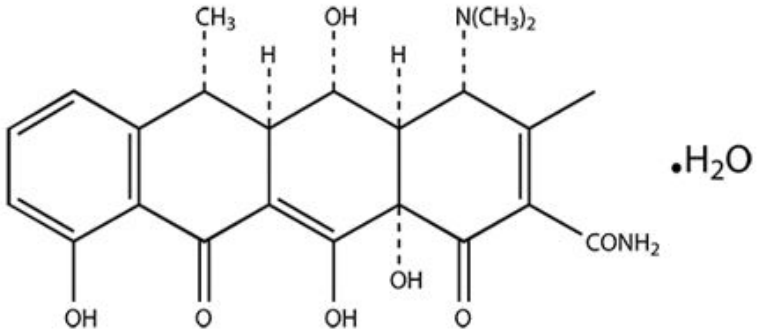


*Figure 22.* Chemical structure of doxycycline monohydrate (biomol).

Kirby-Bauer test, or also called agar diffusion assay, requires the use of petri dishes, nutrient agar, E. coli K-12 bacteria, L-Shaped Cell Spreaders, parafilm, Lysogeny Broth (LB), micropipette, tips, vials, incubator and refrigerator, gloves and lab coat. The most important material for this experiment are Escherichia coli K-12 (E.coli K-12) and LB. E.coli K-12 strain was obtained from Carolina Biology (Burlington, NC). It is gram negative bacteria and kept at 37 $^0C$. Lysogeny Broth is the nutrient for E. Coli K-12. The petri dishes and agar nutrient are from Worldwide Life Science Company too.

**4.2.2 Geometry of the femoral implant**. The geometry of the femoral implant was created in SOLIDWORKS (see Fig. 23) and closely mimics the geometry of an implant used in clinical practice.

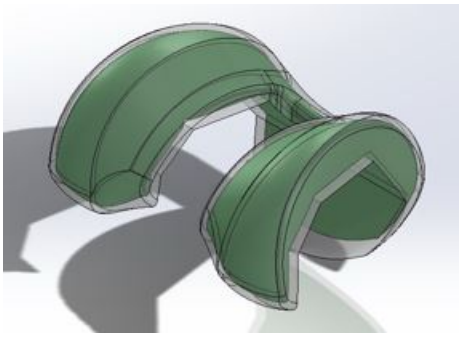

*Figure 23.* 3D model of the femoral implant.

As a novelty, reservoirs and microchannels were introduced within the implant geometry as described in Ranganathan et al. [2]. The micro-channels were placed on the sides, top and the bottom and were connected to two reservoirs (see Fig. 24). The doxycycline solution was introduced into the reservoir through the side hole.

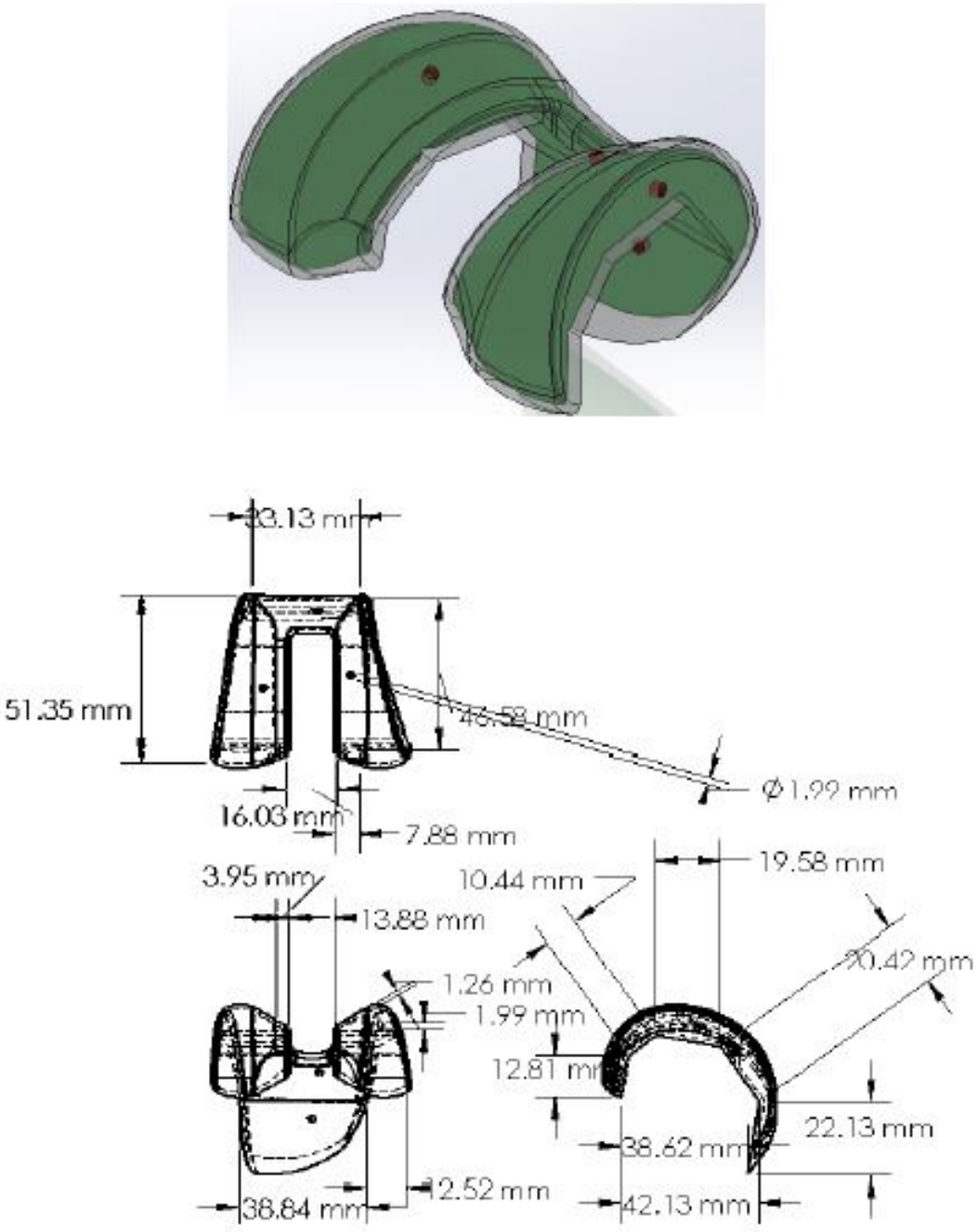


*Figure 24.* Femoral implant with built-in features such as reservoir and five microchannel.

### 4.2.3 3D printing of PCL, PLA and Ti-6Al-4V implants.

***PCL implants***. The main goal is to show the antibiotic loaded 3D printed femoral components are capable of killing bacteria. This will be achieved by first creating 3D printed parts using the geometry of the knee implant shown in Fig. 24. Thereby, we propose manufacturing PCL filament mixed with doxycycline. The diameter of PCL will be between 2.40 and 2.90 mm. Moreover, we propose mixing PCL powders, which represents 75% of total mass of PCL filament, and PCL pellets, which represents 25% of total mass and adding doxycycline representing 0.8% of total mass in an extruder heated to 70 $^0$C. The filament created will be implemented into the 3D printer.

The Ultimaker 2 is the platform through which the 3D printing process is conducted. This process needs to be carefully monitored throughout, as PCL is not an easy material to utilize due to its soft, pliable, properties when heated above room temperature. For this reason, certain parameters within the file and printer settings must be modified in order to ensure good print quality. First, line code should be introduced into the printer's numerical control programming language (G.code) to allow the change of temperature for the nozzle. Second, the implant should be printed at 75% of full scale. This change should be done in Cura, 3D printing software. Third, several parameters in the printer have to be altered: the speed and the temperature should be decreased (temperature of printing PCL should be 130 $^0C$ compared to the standard temperature 210 $^0C$ used for polymers such as poly-lactic acid) while the material flow should be increased by 50% more than the standard flow. Fig. 25 shows the PCL implant with antibiotics infused.

*Figure 25.* PCL implant with antibiotic loaded.

***PLA implants***. The PLA implant were created following the geometry model shown in Fig. 24. The infill of printing was 5%, the height of layers was 0.1 mm and the speed of printing was 60 mm/s. Fig. 26 shows the PLA implant.

*Figure 26.* PLA implant.

***Metal implants***. The metal implant was created using additive manufacturing technique from the third party company TECOMET. The 3D printing technique used is called Direct Metal Laser Sintering. The process requires melting the powder titanium Ti-6Al-4V using the laser. After finishing the creation and letting some time for cooling down, the inside powder are taken off. Fig. 27 shows metal implant.

*Figure 27.* Metal implant.

**4.2.4 Preparation of antibiotic solution**. The 31.6 mg/mL of the doxycycline solution was made by mixing 1.892 ± 5% grams of doxycycline monohydrate in 60 mL of saline, also called 0.9% sodium chloride irrigation, USP shipped from Baxter. Each 100 mL of the solution contain 900 mg of sodium chloride and the pH is between 4.5 and 7.0 with a mean of 5.5. It was made around 20 days before the experiment with a density of 0.976 g/mL.

**4.2.5 Design of experiments**. Before starting the experiment, it is highly recommended to have a 1 L and 255 mL of beaker, saline, doxycycline solution, Titanium, PCL and PLA implants ready. As for PCL, we submerge the implant mixed with doxycycline in beaker filled with 255 mL of saline. The samples were taken in matter of hours. Fig. 28 shows the design of experiment for PCL implant.

*Figure 28.* Design of experiment for PCL implant.

As for PLA and titanium implants, the mass of Titanium (39.44g ± 0.95%) and of PLA (14.134 g ±1.57%) was measured to be able to monitor the total volume of the injected antibiotic solution inside of the reservoirs in each implant. The next step will be filling 1L beaker with saline until reaching the full size then close all microchannel except the side using blue tape 3M to inject antibiotic solution into the implant through the open microchannel using 5 mL syringe. This step will be repeated until the antibiotics solution overflows from the implant. In our records, 8.874 mL ± 5.07% was injected in PLA and 11.58 mL ± 3.61% was injected in Titanium implant which was validated after measuring the final mass of Titanium and PLA implants and divide it with the density of the doxycycline solution. Finally, raise the implant over the open 1L saline filled beaker and remove the tape. Subsequently, lower implant into the beaker to submerge it. 2mL from the sample were taken at different time period. A control experiment was done to investigate the kill radius by repeating

the same experiment without injecting antibiotics solution inside of the implant to confirm the source of the zone inhibition.

## 4.3 Results and Discussions

**4.3.1 Minimum inhibitory concentration (MIC)**. The Kirby-Bauer test is very important for two main reasons: bacteria's sensitivity to antibiotics and MIC. According to Centers of Disease Control and Prevention, most of E. coli are harmless but some of them could be pathogenic [63]. The MIC experiment is very important because it helps understanding and predicting the minimum concentration of antibiotic that can be used.

Finding the MIC requires testing different concentration of doxycycline monohydrate mixed with deionized water to find the zone inhibition. The concentration to be tested are between 0.01 and 4 mg/mL. The first zone inhibition was detected at concentration 0.01 mg/mL. Thereby, we consider 0.01 mg/mL as MIC of doxycycline on E.coli k12 as shown in Fig. 29. Doxycycline hydrochloride mixed with water has a MIC between 0.03-128 mg/L (0.0003-0.128 mg/mL) on Haemophilus species but have a MIC between 0.25-16 mg/L on Neisseria species [60]. Other studies show that the MIC of doxycycline on E. Coli ATCC 25922 is 1 mg/L and no MIC on E. Coli ATCC 35218 compared to 100 mg/L of our MIC on E. Coli ATCC 10798 [64]. Based on these results, our MIC is within these ranges.

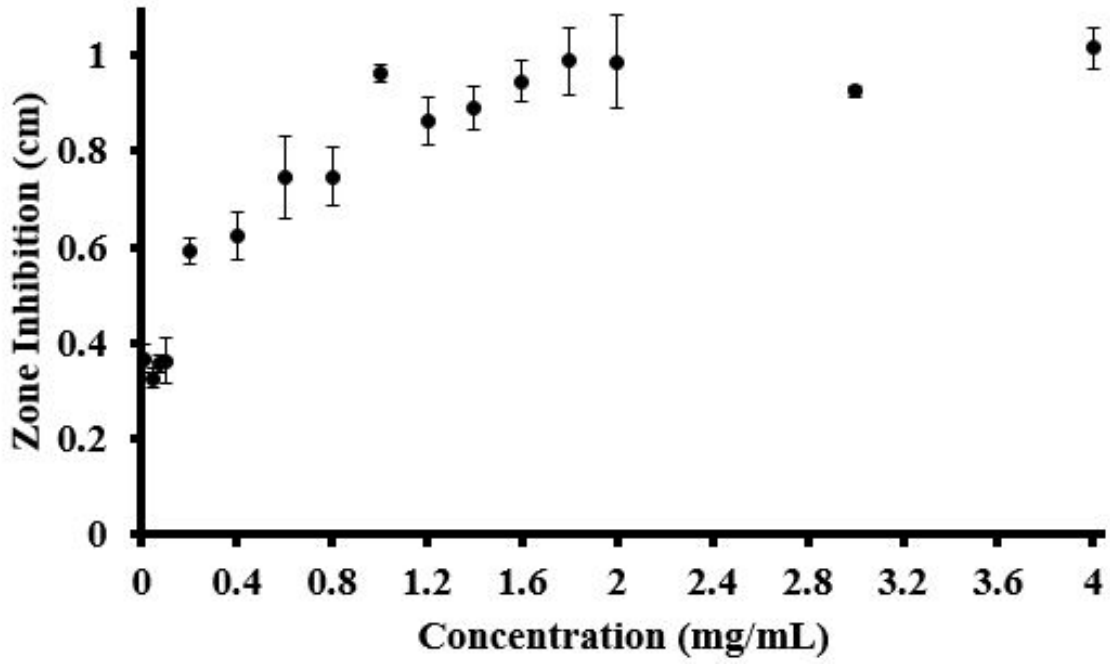


*Figure 29.* MIC curve.

The MIC was also numerically predicted using COMSOL. The process was investigated in 2D. Two circles were built. The first one has a diameter of 100 mm representing petri dishes and the second has a diameter of 6 mm representing filter paper. The small circle is located in the middle of the petri dish. The concentration of the small circle is equivalent of the concentration used for MIC experiment. The concentration of the biggest circle was set to be zero and the uniform diffusion chosen is D=1.5 $\times$ $10^{-11}$ $m^2$/s. The mesh used is free quadrilateral with extra fine size. Fig. 30 shows the mesh of the geometry and result found numerically.

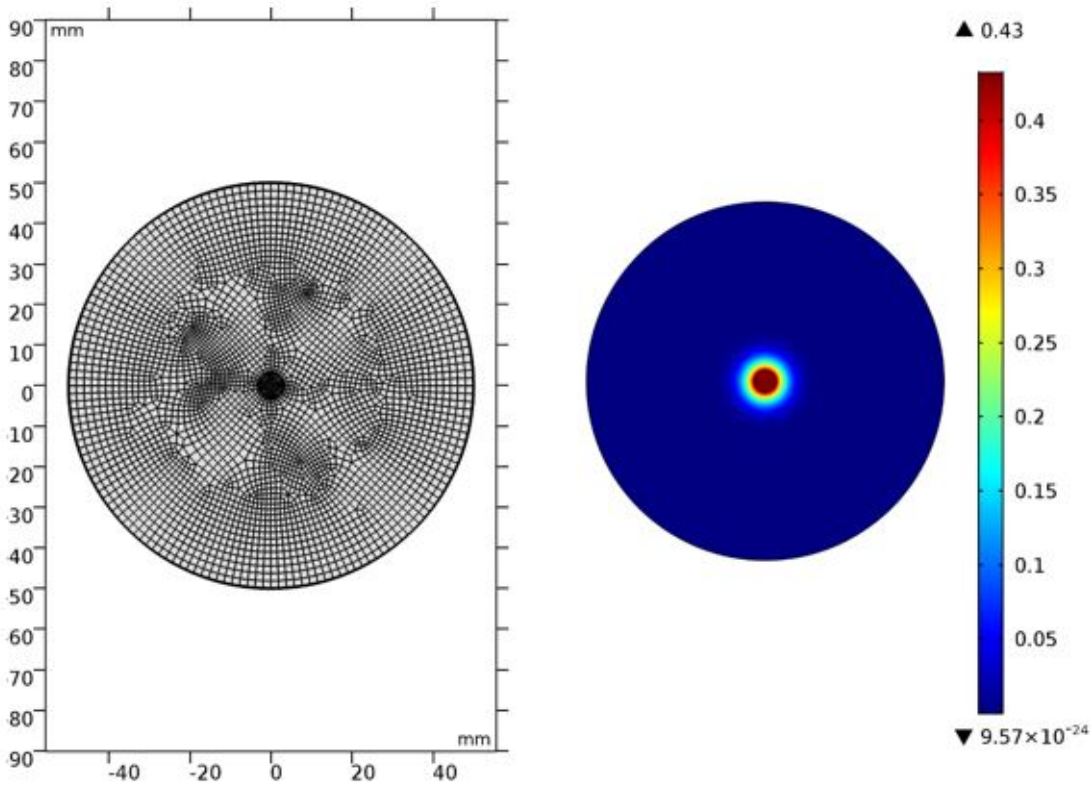


*Figure 30.* Mesh of the geometry and result at c=0.2 mg/mL.

The numerical MIC was validated with experimental result as shown in Fig. 31. We tested the results between 0.2 mg/mL and 1 mg/mL. The outcome shows a very small difference except at 1 mg/mL. In fact, the numerical studies is within the standard deviation of the experimentation. Unfortunately, the higher the concentration, the higher the gap between numerical and experimental results. We hypothesize that Kirby-Bauer test is a medium to medium test but COMSOL works on continuous medium.

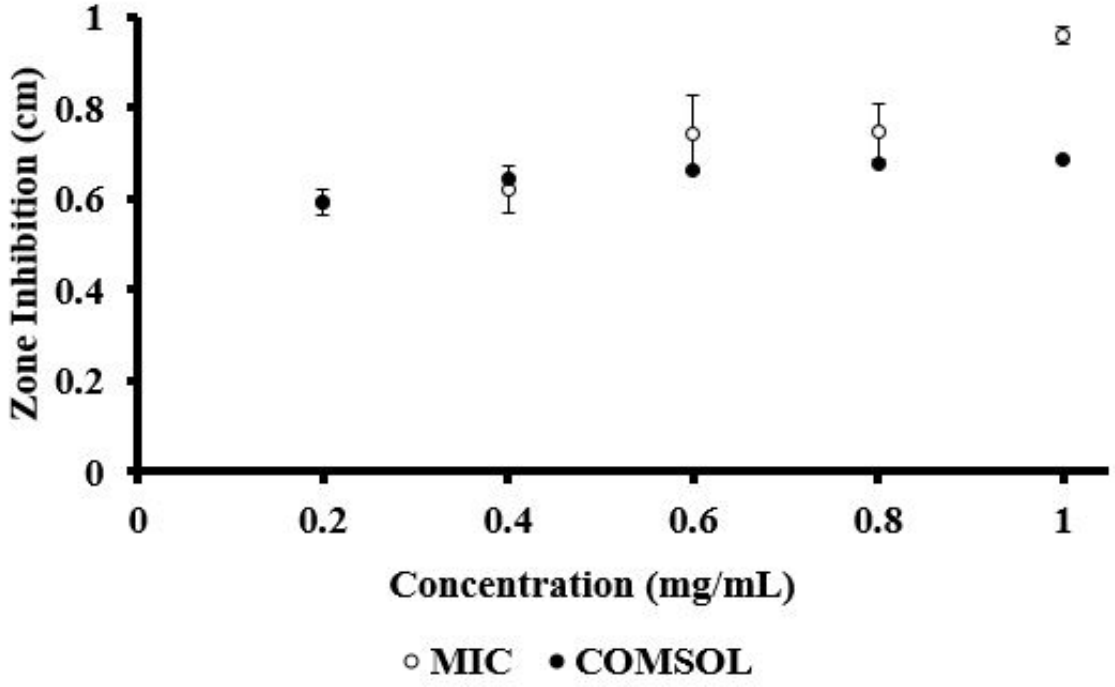


*Figure 31.* Validation of MIC using experimental and numerical work.

**4.3.2 Elution through PCL implants**. For the PCL experiment, a Kirby-Bauer test was implemented to understand the presence and antibacterial abilities of the eluted doxycycline through PCL implants by taking 11 samples from the experiment and detect its zone inhibition. Fig. 32 shows the result of the PCL experiment after 5 and 10 hours and shows the elution of doxycycline through PCL implants. The elution of doxycycline started within the first minutes of the beginning of the experiment. After 9 minutes, the zone inhibition of doxycycline in the saline was 0.9 cm. After 24 hours, the radius was more than 1 cm. Fig. 32 proves the potential of elution within 24 hours. In fact, the zone inhibition can be see even after 5 hours. Moreover, the zone inhibition indicates that the antibiotic elution was still

successful. Contrary to bone cement, even though the implant was heated during manufacturing, doxycycline was still able to kill the bacteria.

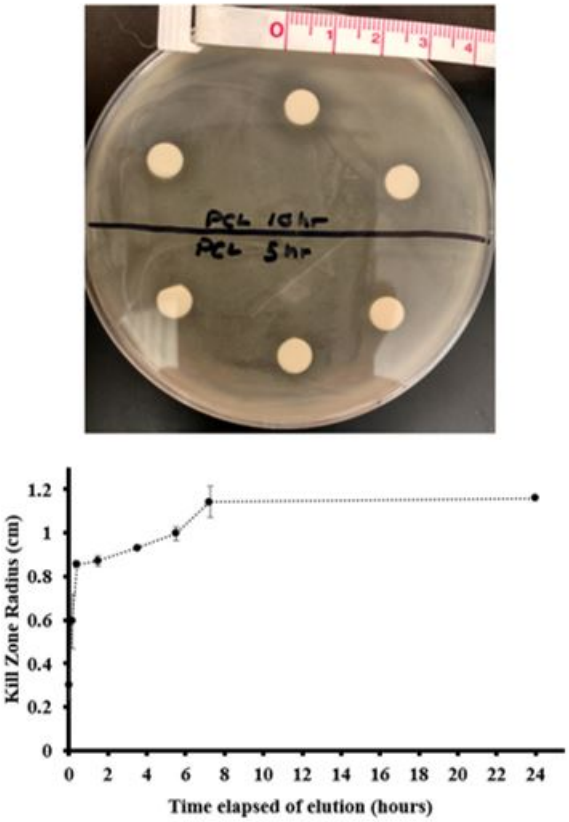


*Figure 32.* Zone inhibition of PCL after 5 and 10 hours experiment and the elution graph of Doxycycline Hyclate from PCL femoral implant.

**4.3.3 Elution through PLA and Ti-6Al-4V implants**. The drug elution through PLA and Ti-6Al-4V implants were evaluated through zone inhibition. Fig. 33 **A** shows the zone inhibition through Ti-6Al-4V. The experiment was run three times. For each experiment, three filter paper were submerged in the solution to get an average zone inhibition with standard deviation. Fig. 33 **B** represents the kill radius of eluted doxycycline through PLA. The procedure is similar to the experiment made on titanium. Appendix B to E represents the result for each experiment after 3 runs.

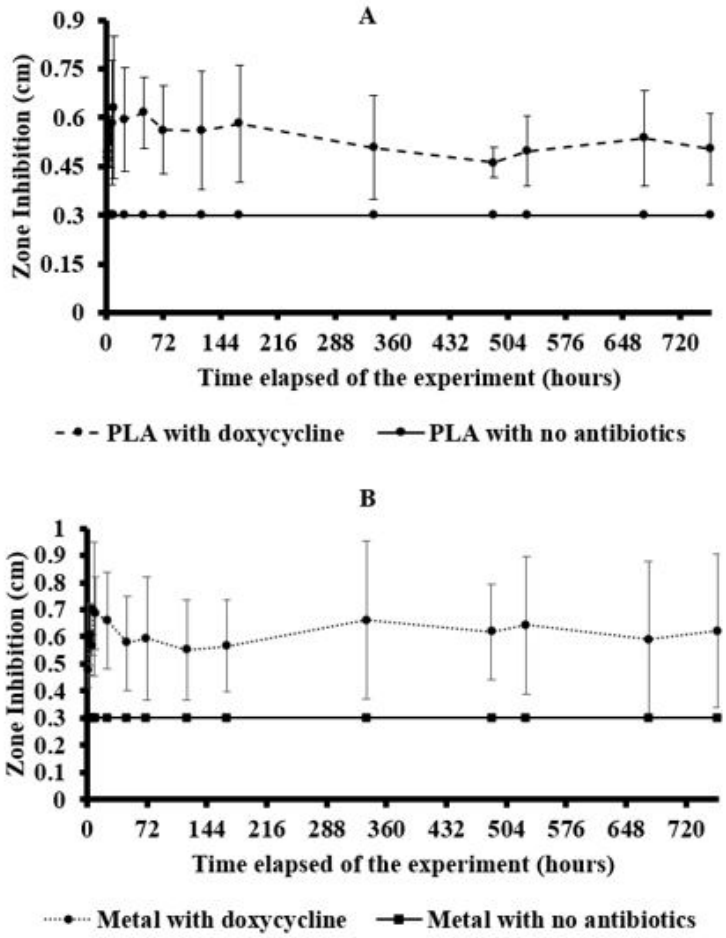


*Figure 33.* Kill Radius of doxycycline eluted through **A** Titanium implant **B** PLA implant.

The control experiment shows no zone inhibition (0.3 cm is the radius of filter used). Thereby, the radius shown in Fig. 33 shows the presence of doxycycline in saline. The median kill radius of PLA experiment is 0.543 cm with standard error of 0.013 and 95% confidence interval of 0.0267. As for metal experiment, the median kill radius is 0.608 cm with standard error of 0.014 and 95% confidence interval of

0.044. According to the confidence, the median of the antibiotic elution from PLA is bounded between 0.516 cm and 0.569 cm and Titanium is bounded between 0.578 cm and 0.638 cm. Fig. 34 shows the 95% confidence interval of PLA and Titanium experiment.

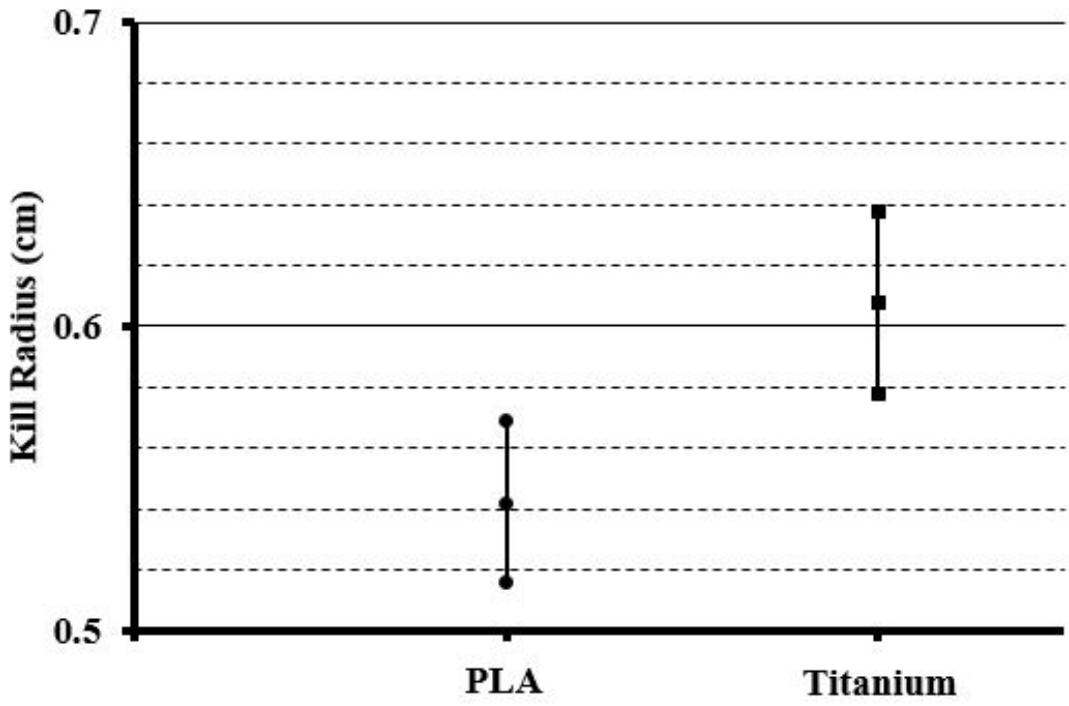


*Figure 34.* Confidence interval of 95% for PLA and Titanium.

The line representing mean interval is considered to be small (less than 0.1 cm for both of them). However, the interval for Titanium is slightly higher than the one

of PLA. Indeed, the maximum value of the mean for PLA is closer to the minimum value of the mean for Titanium. The range of difference of kill radius for PLA experiment is 0.168 cm compare to 0.225 cm for Titanium experiment. Additionally, PLA experiment has a variance of 0.0025 and metal has a variance of 0.0032. These results are small which implies that there is small fluctuation for the two experiments and are in steady-state level.

The comparison between PLA and Titanium experiment was suggested to further investigate the drug release. Fig. 35 shows the column comparing the kill radius at each hour that the samples were taken in the experiment. Fig. 36 shows the comparison of radius between PLA and titanium. The column proves that the doxycycline is released more from titanium than in PLA apart from 1 hour, 120 hours and 168 hours. This was done for two main reasons. First, Titanium has more microchannel than PLA since two more holes are included in titanium implant during fabrication to clean the femur from the powders. Second, we were able to inject 11.58 mL of doxycycline solution in titanium implant compare to 9 mL injection in PLA implant. Fig. 36 confirms the results found in Fig. 35. In Fig. 36, the two graphs are close to stability with small fluctuation after 1 day of experiment. Thus, the drug elution from PLA and Titanium reaches steady-state situation after one day of experiment and stays stable for 30 days.

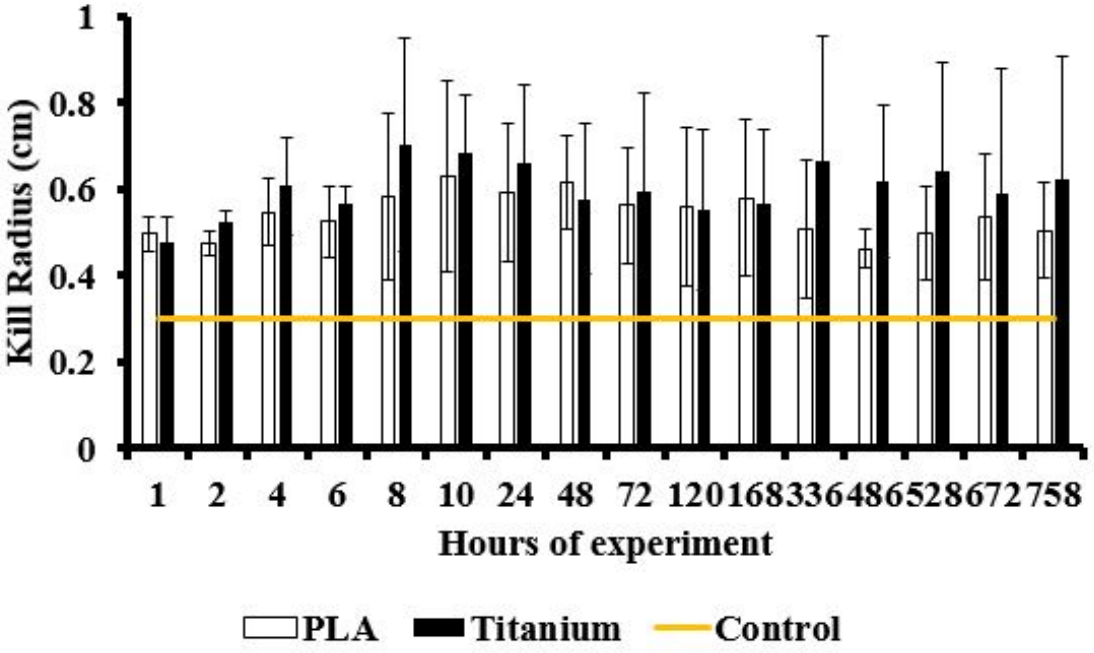


*Figure 35.* Comparison of kill radius of doxycycline eluted from PLA and Titanium at each time taken.

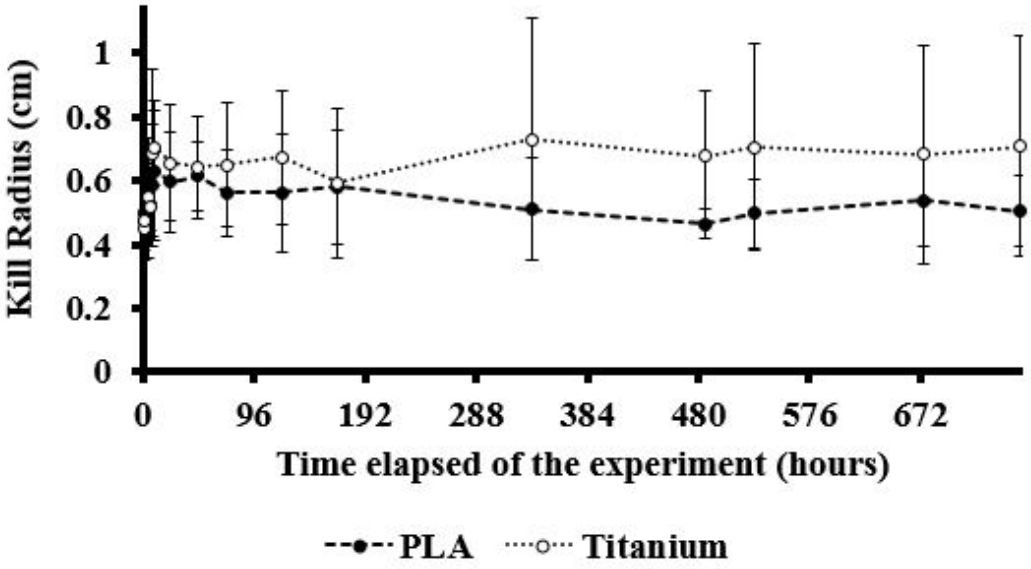


*Figure 36.* Drug elution from PLA Vs Titanium implant.

### 4.4 Summary

In summary, the study of active implant using 3D printing PCL, PLA and Titanium can be a great asset in orthopaedic. In fact, doxycycline eluted through the three materials. Unlike bone cement, the drug elution through PLA and Titanium stayed in steady-state situation for a period of one month after 24 hours. The Kirby-Bauer test is very useful to investigate antibiotic elution and test the ability of antibiotics on bacteria. In this study, the eluted doxycycline demonstrated the ability of killing bacteria. Nevertheless, the experiments were proven to be successful. It is preferable to detect the concentration of doxycycline in saline. Moreover, in-vivo study will be helpful on investigating its application on human body.

# Chapter 5

## Conclusion and Future Research Directions

In this thesis, we investigated the efficacy of eluted antibiotics in 3D printed orthopaedic implants using Titanium (Ti6Al4V), Poly-lactic acid (PLA) and Poly-Caprolactone (PCL) materials.

Chapter 2 focused on the effect of temperature and ultra-violet light on the efficacy of eluted antibiotics. Results indicate that the exposure to temperature had little effect on the efficacy of doxycycline, vancomycin and cefazolin. However, UV light did adversely impact the efficacy of vancomycin. Thereby, SLA printing may not be appropriate to print implants infused with vancomycin but FDM printing can be used for all antibiotics considered in this research.

The elution of doxycycline through cubic shaped implant with built-in reservoir was investigated in Chapter 3. Experiments were conducted using HPLC and were used to calibrate the numerical model in COMSOL. Results indicated that the retention time of doxycycline was found around 9.56 min. Furthermore, 70 % of doxycycline was released in 15 days.

Chapter 4 investigated the elution of doxycycline through 3D printed femoral implants with built-in reservoir and microchannels using three different materials: Poly-Lactic Acid (PLA), Poly-Caprolactone (PCL) and Titanium grade Ti-6Al-4V. The antibacterial ability of eluted doxycycline from PCL, PLA and Titanium were inspected using Kirby-Bauer test on the bacteria E.coli k-12. Results show that most of doxycycline eluted through the three materials in the first 24 hours and reached the steady-state level after 30 days for PLA and Titanium. Additionally, Titanium implants released more amount of antibiotics than the ones made using PLA.

Results from the present study highlight the potential of using 3D printed polymeric and metallic implants with built-in reservoir(s) and microchannel(s)

in orthopaedic applications. In the future, additional experiments are necessary to understand the variability observed in the obtained results. It would also be preferable to conduct in-vivo experiments to further investigate the drug elution and examine the possible side effects. Also, a complete Finite Element Model of the 3D femoral implant can be set up to optimize the implant geometry that could potentially minimize the total number of experimental trials required to bring this promising concept to market.

## References


[1] S. Weinstein, S.I.W Castillo and E. Yelin. (2018) By The Numbers - Musculoskeletal Conditions: The Big Picture.

[2] S.I. Ranganathan, T.W.B Kim, D.J. Campbell, G.C. Smith, "Novel biodegradable and non-biodegradable 3d printed implants as a drug delivery system," jun 2018, US Patent App. 15/736,885.

[3] C.W. Norden and E. Kennedy, "Experimental osteomyelitis. II. Therapeutic trials and measurement of antibiotic levels in bone," Journal of Infectious diseases, vol. 124, pp. 565–571, 1971.

[4] K.Y. Ha, Y.G. Chung, and S.J. Ryoo,"Adherence and biofilm formation of staphylococcus epidermidis and mycobacterium tuberculosis on various spinal implants," *Spine*, vol. 30, pp. 38–43, 2005.

[5] E. Sheehan, J. McKenna, K. Mulhall, P. Marks, and D. McCormack, "Adhesion of staphylococcus to orthopaedic metals, an in vivo study," *Journal of Orthopaedic Research*, vol. 22, pp. 39–43, 2004.

[6] R. O. Darouiche, A. Dhir, A. J. Miller, G. C. Landon, I. I. Raad, and D.M. Musher, "Vancomycin penetration into biofilm covering infected prostheses and effect on bacteria," *Journal of Infectious Diseases*, vol. 170, pp. 720–723, 1994.

[7] G. H. Walenkamp, L. L. Kleijn, and M. de Leeuw, "Osteomyelitis treated with gentamicin-PMMA beads: 100 patients followed for 1–12 years," *Acta Orthopaedica Scandinavica*, vol. 69, pp. 518–522, 1998.

[8] J. D. Blaha, J. H. Calhoun, C. L. Nelson, S. L. Henry, D. Seligson, J. J. Esterhai, R. B. Heppenstall, J. Mader, R. P. Evans, and J. Wilkins, "Comparison of the clinical efficacy and tolerance of gentamicin PMMA beads on surgical wire versus combined and systemic therapy for osteomyelitis." *Clinical orthopaedics and related research*, no. 295, pp. 8–12, 1993.

[9] P. Grime, J. Bowerman, and P. Weller,"Gentamicin impregnated polymethylmethacrylate (PMMA) beads in the treatment of primary chronic osteomyelitis of the mandible," *British Journal of Oral and Maxillofacial Surgery*, vol. 28, pp. 367–374, 1990.

[10] S. A. Majid, L. T. Lindberg, B. Gunterberg, and M. S. Siddiki, "Gentamicin-PMMA beads in the treatment of chronic osteomyelitis," *Acta Orthopaedica Scandinavica*, vol. 56, pp. 265–268, 1985.

[11] E. P. Dellinger, S. D. Miller, M. J. Wertz, M. Grypma, B. Droppert, and P.A. Anderson, "Risk of infection after open fracture of the arm or leg," *Archives of Surgery*, vol. 123, pp. 1320–1327, 1988.

[12] R. Johner and O. Wruhs, "Classification of tibial shaft fractures and correlation with results after rigid internal fixation." *Clinical orthopaedics and related research*, no. 178, pp. 7–25, 1983.

[13] D. Paley and J. E. Herzenberg, "Intramedullary infections treated with antibiotic cement rods: preliminary results in nine cases," *Journal of orthopaedic trauma*, vol. 16, pp. 723–729, 2002.

[14] R. Thonse and J. D. Conway, "Antibiotic cement-coated nails for the treatment of infected nonunions and segmental bone defects," *JBJS*, vol. 90, pp. 163–174, 2008.

[15] C.M. Brandt, M.C. Duffy, E.F. Berbari, A.D. Hanssen, J.M. Steckelberg, and D.R. Osmon, "Staphylococcus aureus prosthetic joint infection treated with prosthesis removal and delayed reimplantation arthroplasty," in *Mayo Clinic Proceedings*, vol. 74, 1999, pp. 553–558.

[16] S. J. Volin, S. H. Hinrichs, and K. L. Garvin, "Two-stage reimplantation of total joint infections: a comparison of resistant and non-resistant organisms," *Clinical Orthopaedics and Related Research*, vol. 427, pp. 94–100, 2004.

[17] Y. Mittal, T. K. Fehring, A. Hanssen, C. Marculescu, S.M. Odum, and D. Osmon, "Two-stage reimplantation for periprosthetic knee infection involving resistant organisms," *JBJS*, vol. 89, pp. 1227–1231, 2007.

[18] J. C. Sherrell, T. K. Fehring, S. Odum, E. Hansen, B. Zmistowski, A. Dennos, N. Kalore, P. I. Consortium et al., "The chitranjan ranawat award: fate of two-stage reimplantation after failed irrigation and debridement for periprosthetic knee infection," *Clinical Orthopaedics and Related Research*, vol. 469, pp. 18–25, 2011.

[19] T. Mahmud, M.C. Lyons, D.D. Naudie, S. J. MacDonald, and R.W. McCalden,"Assessing the gold standard: a review of 253 two-stage revisions for infected TKA," *Clinical Orthopaedics and Related Research*, vol. 470, pp. 2730–2736, 2012.

[20] R. Pitto and I. Spika, "Antibiotic-loaded bone cement spacers in two-stage management of infected total knee arthroplasty," *International orthopaedics*, vol. 28, pp. 129–133, 2004.

[21] E. B. Minelli, C. Caveiari, and A. Benini, "Release of antibiotics from polymethylmethacrylate cement," *Journal of chemotherapy*, vol. 14, pp. 492–500, 2002.

[22] K. Anagnostakos and J. Kelm, "Enhancement of antibiotic elution from acrylic bone cement," *Journal of Biomedical Materials Research Part B: Applied Biomaterials*, vol. 90, pp. 467–475, 2009.

[23] K. Anagnostakos, P. Hitzler, D. Pape, D. Kohn, and J. Kelm, "Persistence of bacterial growth on antibiotic-loaded beads: is it actually a problem?" *Acta orthopaedica*, vol. 79, pp. 302–307, 2008.

[24] J. Hendriks, D. Neut, J. Van Horn, H. Van der Mei, and H. Busscher, "Bacterial survival in the interfacial gap in gentamicin-loaded acrylic bone cements", *The Journal of bone and joint surgery*. British volume, vol. 87, pp. 272–276, 2005.

[25] D.J.F. Moojen, B. Hentenaar, H.C. Vogely, A.J. Verbout, R.M. Castelein, and W.J. Dhert, "In vitro release of antibiotics from commercial PMMA beads and articulating hip spacers," *The Journal of arthroplasty*, vol. 23, pp.1152–1156, 2008.

[26] S.B. Kim, Y.J. Kim, T.L. Yoon, S.A. Park, I.H. Cho, E.J. Kim, I.A. Kim, and J.W. Shin, "The characteristics of a hydroxyapatite–chitosan–PMMA bone cement", *Biomaterials*, vol. 25, pp. 5715–5723, 2004.

[27] A.W. Bauer, W.M.M. Kirby, J.C. Sherris, and M. Turck, "Antibiotic susceptibility testing by a standardized single disk method," *American Journal of Clinical Pathology*, vol. 45, pp. 493–496, 1966.

[28] D. Radenkovic, A. Solouk, and A. Seifalian, "Personalized development of human organs using 3d printing technology," *Medical hypotheses*, vol. 87, pp. 30–33, 2016.

[29] M.S. Mannoor, Z. Jiang, T. James, Y.L. Kong, K.A. Malatesta, W.O.Soboyejo, N. Verma, D.H. Gracias, and M.C. McAlpine, "3D printed bionic ears," *Nano letters*, vol. 13, pp. 2634–2639, 2013.

[30] F. Tamimi, J. Torres, U. Gbureck, E. Lopez-Cabarcos, D.C. Bassett, M.H. Alkhraisat, and J.E. Barralet, "Craniofacial vertical bone augmentation: a comparison between 3D printed monolithic monetite blocks and autologous onlay grafts in the rabbit," *Biomaterials*, vol. 30, pp. 6318–6326, 2009.

[31] Y. Zhang, J. Zhu, Z. Wang, Y. Zhou, and X. Zhang, "Constructing a 3D-printable, bioceramic sheathed articular spacer assembly for infected hip arthroplasty," *Journal of Medical Hypotheses and Ideas*, vol. 9, pp. 13–19, 2015.

[32] T. W. B. Kim, O. J. Lopez, J. P. Sharkey, K. R. Marden, M. R. Murshed, and S.I. Ranganathan, "3D printed liner for treatment of periprosthetic joint infections", *Medical hypotheses*, vol.102, pp. 65–68, 2017.

[33] C. L. Ventola, "Medical applications for 3d printing: current and projected uses," *Pharmacy and Therapeutics*, vol. 39,pp. 704, 2014.

[34] M. B. Hoy, "3D printing: making things at the library," *Medical reference services quarterly*, vol. 32, pp. 93–99, 2013.

[35] X. Cui, T. Boland, D. DD'Lima, and M. K Lotz, "Thermal inkjet printing in tissue engineering and regenerative medicine," *Recent patents on drug delivery & formulation*, vol. 6, pp. 149–155, 2012.

[36] R. Stowe, "What is uv curing and what can uv curing do for you?" 2016.

[37] E.P. Holowka and S.K. Bhatia, "Controlled-release systems," in *Drug delivery: materials design and clinical perspective.* Springer, New York, NY 2014, ch. 2, pp. 7–62.

[38] G. Tiwari, R. Tiwari, B. Sriwastawa, L. Bhati, S. Pandey, P. Pandey, and S.K.Bannerjee, "Drug delivery systems: An updated review," *International journal of pharmaceutical investigation*, vol. 2,p. 2, 2012.

[39] R. Langer, "New methods of drug delivery," *Science*, vol. 249, pp. 1527–1533, 1990.

[40] R. Siegel and M. Rathbone, "Overview of controlled release mechanisms," in *Fundamentals and Applications of Controlled Release Drug Delivery*, J. Siepmann, R. Siegel, and M. Rathbone, Eds. Springer US Boston, MA, 2011, ch. 2, pp. 19–43.

[41] C.P. Foley, N. Nishimura, K.B. Neeves, C.B. Schaffer, and W.L. Olbricht, "Flexible microfluidic devices supported by biodegradable insertion scaffolds for convection-enhanced neural drug delivery," *Biomedical microdevices*, vol. 11, p. 915, 2009.

[42] M. Farina, A. Ballerini, G. Torchio, G. Rizzo, D. Demarchi, U. Thekkedath and A. Grattoni, "Remote magnetic switch off microgate for nanofluidic drug delivery implants," *Biomedical microdevices*, vol. 19, p. 42, 2017.

[43] L. Monser and F. Darghouth, "Rapid liquid chromatographic method for simultaneous determination of tetracyclines antibiotics and 6-epi-doxycycline in pharmaceutical products using porous graphitic carbon column", *Journal of pharmaceutical and biomedical analysis*, vol. 23, pp. 353–362, 2000.

[44] J. Fiori, G. Grassigli, P. Filippi, R. Gotti, and V. Cavrini, "HPLC-dad and LC -ESI-MS analysis of doxycycline and related impurities in doxipan mix, a medicated premix for incorporation in medicated feedstuff," *Journal of pharmaceutical and biomedical analysis*, vol. 37, pp. 979–985, 2005.

[45] S. Shariati, Y. Yamini, and A. Esrafili, "Carrier mediated hollow fiber liquid phase microextraction combined with HPLC-UV for preconcentration and determination of some tetracycline antibiotics," *Journal of Chromatography B*, vol. 877, pp. 393–400, 2009.

[46] S. Aldrich, "Separations of tetracycline antibiotics by reversed phase hplc, using discovery columns."

[47] H. Yoshida and M. Nagaoka, "Multiple-relaxation-time lattice boltzmann model for the convection and anisotropic diffusion equation", *Journal of Computational Physics*, vol. 229, pp. 7774–7795, 2010.

[48] E.B. Watson, K.H. Wanser, and K.A. Farley, "Anisotropic diffusion in a finite cylinder, with geochemical applications," *Geochimica et Cosmochimica Acta*, vol. 74, pp. 614–633, 2010.

[49] M. Jamshidian, E.A. Tehrany, M. Imran, M. Jacquot, and S. Desobry, "Poly-lactic acid: production, applications, nanocomposites, and release studies", *Comprehensive Reviews in Food Science and Food Safety*, vol. 9, pp. 552–571, 2010.

[50] S.C. Cox, J.A. Thornby, G.J. Gibbons, M.A. Williams, and K.K. Mallick, "3D printing of porous hydroxyapatite scaffolds intended for use in bone tissue engineering applications," *Materials Science and Engineering: C*, vol. 47, pp. 237–247, 2015.

[51] A. Huesgen, "Agilent 1290 infinity binary LC system with ISET-emulation of a waters", 2014.

[52] J.O. Galante, J. Lemons, M. Spector, P.D. Wilson Jr, and T.M. Wright, "The biologic effects of implant materials," *Journal of orthopaedic research*, vol. 9, pp. 760–775, 1991.

[53] M. A. Woodruff and D. W. Hutmacher, "The return of a forgotten polymer—polycaprolactone in the 21st century," *Progress in polymer science*, vol. 35, pp. 1217–1256, 2010.

[54] K. M. Nampoothiri, N. R. Nair, and R. P. John, "An overview of the recent developments in polylactide (PLA) research," *Bioresource technology*, vol. 101, pp. 8493–8501, 2010.

[55] J. Barksdale, "Encyclopedia of the chemical elements, "titanium"," pp. 732–738, 1968.

[56] K.J. Saleh, M.M. El Othmani, T.H. Tzeng, W.M. Mihalko, M.C. Chambers, and T.M. Grupp, "Acrylic bone cement in total joint arthroplasty: a review", *Journal of Orthopaedic Research*, vol. 34, pp. 737–744, 2016.

[57] S.W. Fage, J. Muris, S.S. Jakobsen, and J.P. Thyssen, "Titanium: a review on exposure, release, penetration, allergy, epidemiology, and clinical reactivity," *Contact Dermatitis*, vol. 74, pp. 323–345, 2016.

[58] Aerospace Specifications Metals Inc. "Titanium Ti-6Al-4V (grade 5), annealed." [Online]

[59] C. S. Adams, V. Antoci Jr, G. Harrison, P. Patal, T.A. Freeman, I.M. Shapiro, J. Parvizi, N.J. Hickok, S. Radin, and P. Ducheyne, "Controlled release of vancomycin from thin sol-gel films on implant surfaces successfully controls osteomyelitis", *Journal of Orthopaedic Research*, vol. 27, pp. 701–709, 2009.

[60] D. Neut, J. G. Hendriks, J. R. van Horn, R. S. Kowalski, H. C. van der Mei and H. J. Busscher, "Antimicrobial efficacy of gentamicin-loaded acrylic bone cements with fusidic acid or clindamycin added," *Journal of orthopaedic research*, vol. 24, pp. 291–299, 2006.

[61] S. Rossi, A. O. Azghani, and A. Omri, "Antimicrobial efficacy of a new antibiotic-loaded poly (hydroxybutyric-co-hydroxyvaleric acid) controlled release system," *Journal of antimicrobial chemotherapy*, vol. 54, pp. 1013–1018, 2004.

[62] J. M. Andrews, "Determination of minimum inhibitory concentrations," *Journal of antimicrobial Chemotherapy*, vol. 48, pp. 5–16, 2001.

[63] CDC, "E.coli (escherichia coli)," Feb 2018. [Online].

[64] E. C. for Antimicrobial Susceptibility Testing (EUCAST) of the European Society of Clinical Microbiology and I. D. (ESCMID), "Determination of minimum inhibitory concentrations (mics) of antibacterial agents by broth dilution," *Clinical Microbiology and Infection*, vol. 9, pp. ix–xv, 2003.

## Appendix A

## Retention Time of Doxycycline Detected in High Performance Liquid Chromatography (HPLC)

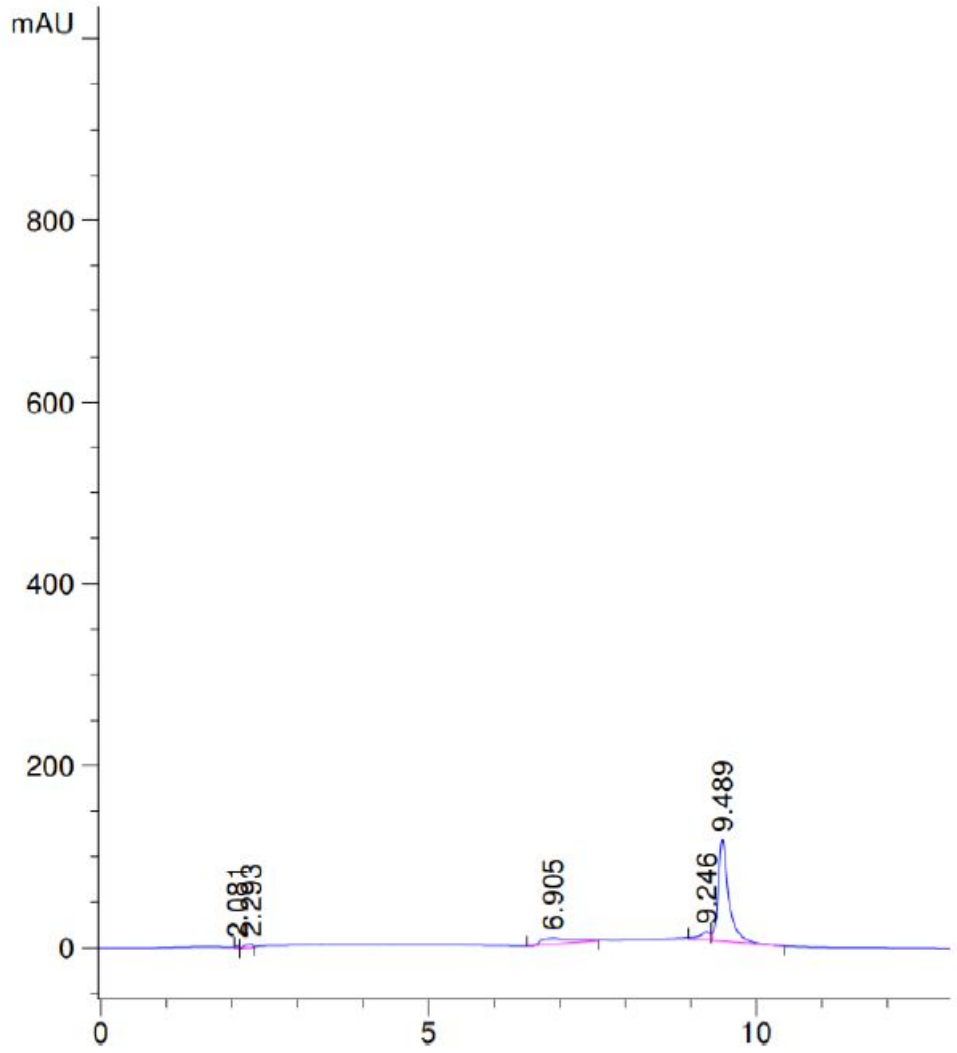


*Figure A1.* Detection of doxycycline in ethanol solution when injection is 1 $\mu$L.

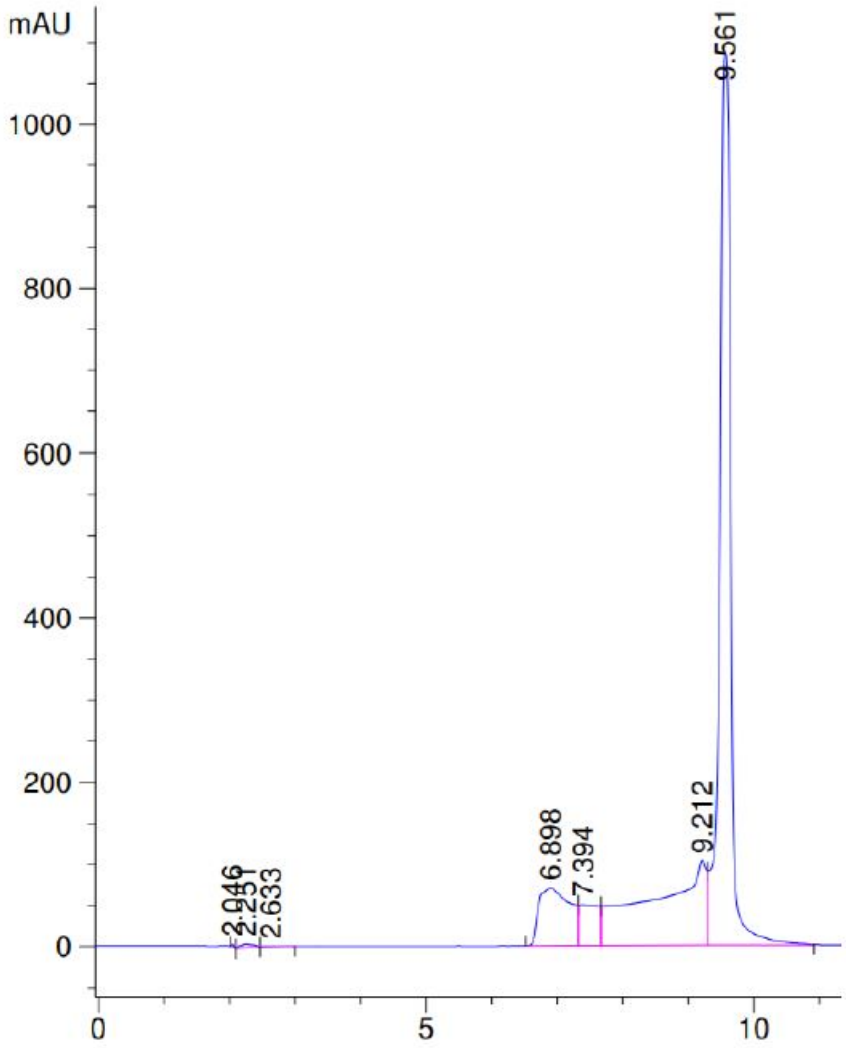


*Figure A2.* Detection of doxycycline in ethanol solution when injection is 5 $\mu$L.

## Appendix B

## Poly (lactic acid) (PLA) - Doxycycline Monohydrate 31.6 mg/mL

Table B1

*Zone Inhibition and Standard Deviation of release of Doxycycline from PLA implant*

| Time(hours) | Radius kill (cm) | Standard Deviation |
|---|---|---|
| 1 | 0.496 | 0.042 |
| 2 | 0.475 | 0.027 |
| 4 | 0.546 | 0.077 |
| 6 | 0.525 | 0.081 |
| 8 | 0.584 | 0.191 |
| 10 | 0.630 | 0.220 |
| 24 | 0.595 | 0.160 |
| 48 | 0.614 | 0.108 |
| 72 | 0.563 | 0.136 |
| 120 | 0.561 | 0.183 |
| 168 | 0.581 | 0.180 |
| 336 | 0.509 | 0.161 |
| 486 | 0.463 | 0.046 |
| 528 | 0.497 | 0.107 |
| 675 | 0.537 | 0.146 |
| 758 | 0.504 | 0.110 |

## Appendix C

## Poly (lactic acid) (PLA) - No Antibiotic

Table C1

*Zone Inhibition and Standard Deviation on PLA implant with no antibiotics*

| Time(hours) | Radius kill (cm) | Standard Deviation |
|---|---|---|
| 1 | 0.3 | 0 |
| 2 | 0.3 | 0 |
| 4 | 0.3 | 0 |
| 6 | 0.3 | 0 |
| 8 | 0.3 | 0 |
| 10 | 0.3 | 0 |
| 24 | 0.3 | 0 |
| 48 | 0.3 | 0 |
| 72 | 0.3 | 0 |
| 120 | 0.3 | 0 |
| 168 | 0.3 | 0 |
| 336 | 0.3 | 0 |
| 486 | 0.3 | 0 |
| 528 | 0.3 | 0 |
| 675 | 0.3 | 0 |
| 758 | 0.3 | 0 |

## Appendix D

## Titanium Ti6Al4V - Doxycycline Monohydrate 31.6 mg/mL

Table D1

*Zone Inhibition and Standard Deviation of release of Doxycycline from Ti6Al4V implant*

| Time(hours) | Radius kill (cm) | Standard Deviation |
|---|---|---|
| 1 | 0.476 | 0.060 |
| 2 | 0.590 | 0.132 |
| 4 | 0.608 | 0.113 |
| 6 | 0.568 | 0.038 |
| 8 | 0.702 | 0.247 |
| 10 | 0.687 | 0.133 |
| 24 | 0.662 | 0.178 |
| 48 | 0.577 | 0.173 |
| 72 | 0.595 | 0.227 |
| 120 | 0.553 | 0.184 |
| 168 | 0.566 | 0.171 |
| 336 | 0.663 | 0.292 |
| 486 | 0.619 | 0.176 |
| 528 | 0.643 | 0.252 |
| 675 | 0.591 | 0.289 |
| 758 | 0.622 | 0.284 |

## Appendix E

## Titanium Ti6Al4V - No Antibiotic

Table E1

*Zone Inhibition and Standard Deviation on Ti6Al4V implant with no antibiotics*

| Time(hours) | Radius kill (cm) | Standard Deviation |
|---|---|---|
| 1 | 0.3 | 0 |
| 2 | 0.3 | 0 |
| 4 | 0.3 | 0 |
| 6 | 0.3 | 0 |
| 8 | 0.3 | 0 |
| 10 | 0.3 | 0 |
| 24 | 0.3 | 0 |
| 48 | 0.3 | 0 |
| 72 | 0.3 | 0 |
| 120 | 0.3 | 0 |
| 168 | 0.3 | 0 |
| 336 | 0.3 | 0 |
| 486 | 0.3 | 0 |
| 528 | 0.3 | 0 |
| 675 | 0.3 | 0 |
| 758 | 0.3 | 0 |